Drowsiness Prognosis Using Chaos Theory

by

Behzad Abdi

M.A.Sc., Simon Fraser University, 2012

MA.Sc., Tehran Azad University, 1999

B.Sc., Iran University of Science & Technology, 1993

Thesis Submitted in Partial Fulfillment of the
Requirements for the Degree of
Doctor of Philosophy

in the
School of Mechatronic Systems Engineering
Faculty of Applied Sciences

SIMON FRASER UNIVERSITY
Spring 2023

Declaration of Committee

Name:	**Behzad Abdi**
Degree:	**Doctor of Philosophy**
Title:	**Drowsiness Prognosis Using Chaos Theory**
Committee:	**Chair: Amr Marzouk** Senior Lecturer, Mechatronic Systems Engineering **Farid Golnaraghi** Supervisor Professor, Mechatronic Systems Engineering **Siamak Arzanpour** Committee Member Associate Professor, Mechatronic Systems Engineering **Krishna Vijayaraghavan** Committee Member Associate Professor, Mechatronic Systems Engineering **Majid Shokoufi** Examiner Lecturer, Engineering Science **Shahab Ghafari** External Examiner Associate Dean, Applied Technology Humber College

Ethics Statement

The author, whose name appears on the title page of this work, has obtained, for the research described in this work, either:

a. human research ethics approval from the Simon Fraser University Office of Research Ethics

or

b. advance approval of the animal care protocol from the University Animal Care Committee of Simon Fraser University

or has conducted the research

c. as a co-investigator, collaborator, or research assistant in a research project approved in advance.

A copy of the approval letter has been filed with the Theses Office of the University Library at the time of submission of this thesis or project.

The original application for approval and letter of approval are filed with the relevant offices. Inquiries may be directed to those authorities.

Abstract

Drowsiness is a state of impaired awareness or decreased consciousness related to a desire or inclination to sleep and difficulty in remaining alert [1]. It is considered one of the leading causes of truck accidents in the mining industry, causing irrecoverable economic, health, and life losses. An intelligent prognosis system can help the mining industry save the operator's life and expensive mining instruments. Despite the significant progress in drowsiness detection in recent years, the reliable early prognosis of drowsiness is still challenging. Electrocardiogram (EEG) base drowsiness detection method is a reliable approach that may be implemented by applying wearable devices [3]. This research aims to discover accurate fractal dimension and entropy algorithms that can be applied to EEG signals to compute reliable and effective indices for early drowsiness prognosis. Our approach takes advantage of chaotic quantifiers, including fractal dimension and entropy indices for feature extraction from EEG signal during the alert to a drowsy state transition. To accomplish this, a thorough analysis and evaluation were undertaken to examine the sensitivity and robustness of chaotic indicators, which included five fraction dimension algorithms and four main entropy approaches in terms of their capacity to forecast early drowsiness. According to the extracted feature evaluation, Higuchi and Katz's fraction dimension, Fuzzy and Permutation entropy indices perform better in discriminating alert and drowsy states. In this study, we utilized the fusion of different indicators for the proposed classifier. We trained and tested an SVM classifier that provided high performance by selecting a compact set of features that offer the greatest differentiability between the alert and drowsy states. Experiment results reveal that based on four fractal dimensions and entropy fusion, our strategy improves classification performance in distinguishing between the alert and drowsy states, with an accuracy of 96.30%.

Keywords: Chaos; Drowsiness; EEG, Nonlinear Analysis, Fractal Dimension, Entropy

Dedication

Dedicated to my lovely wife, Bita Ebadian

my parents and my daughters

Roank, Ava, Anissa

for your support and encouragement

Acknowledgements

My sincere thanks and gratitude to my senior supervisor, Dr. Farid Golnaraghi, who has given me this opportunity to work with him and provided continuous support and valuable guidance during my Ph.D. study. His insightful comments and suggestions helped me keep on the right way of researching. Above all, he gave me constant encouragement and support in my research activities. I take this opportunity to thank my thesis committee, Dr. Siamak Arzanpour and Dr. Krishna Vijayaraghavan, for agreeing to be on my advisory committee, giving me constructive advice, and spending time reviewing my work. I would also like to thank the examining committee, Dr. Shahab Ghafari and Dr., and the session chair, Dr., for agreeing to be a part of my thesis defence. At this moment, I express my sincere thanks to the staff of Mechatronic Systems Engineering at Simon Fraser University for being friendly and supportive.

Special thanks to everyone who served as subjects for our clinical studies or others who, in one way or another, helped me to conduct this research.

Table of Contents

List of Tables

List of Figures

Chapter 1.

Introduction

1.1. Background and Motivation

Mining is a US$700+ billion industry that uses large machinery to excavate and transport commodity materials [53]. Most mining industry equipment, such as mining haul trucks and excavators, require significant investments; for instance, mining trucks cost around US$4 million each, and shovels around US$10 million each [53]. Any human error could be a significant obstacle to companies' profitability that utilizes such machinery as they cause unexpected equipment downtime and losses. Humans operate most mining equipment, and their monotonous and repetitive tasks lead the operators to fall asleep. In open-pit mines, drowsiness-related accidents alone account for about 65% of truck driving accidents [79]. The company's assets' total loss is around US$22.6 billion, and operator lives are not replaceable [78, 79]. The lack of real-time drowsiness monitoring and prognosis in the mining industry can cause irrecoverable losses. If drivers and industrial operators are warned in time, about 90% of drowsiness-related accidents may be avoided [79]. Hence, an intelligent drowsiness prognosis system is vital in the mining industry to save the operator's life and expensive mining instruments.

Current research on drowsiness detection can be grouped into three main categories: vehicle-based, behavioural-based, and physiological-based measurements. Behaviour-based and vehicle-based drowsiness detection methods are unreliable and lose their effectiveness outside laboratory settings due to environmental circumstances, road geometry, and driving conditions [3]. Meanwhile, they detect drowsiness when the driver starts to sleep, which is often too late to prevent an accident, so they are not considered early drowsiness prognosis tools [7]. Physiological-based measurements use physiological parameters such as heart rate, respiration rate, blood pressure, and brain signals to detect drowsiness. The brain's electrical signals (electroencephalogram – EEG) strongly correlate with drowsiness and are considered reliable and precise drowsiness indicators [14]. Among the mentioned techniques, drowsiness prognosis using EEG signal is a golden key. Current drowsiness detection methods utilize linear EEG analysis, whereas the brain signals are nonstationary and nonlinear [6]. Linear analysis of brain signals in some applications, ignores EEG signals' nonlinear behaviour that leads to reliability and accuracy loss in drowsiness prediction [7].

In this thesis, we propose research to develop an accurate, wearable, and cost-effective drowsiness forecasting system that utilizes nonlinear data processing using chaos theory for the mining industry.

1.2. Current Drowsiness Detecting Techniques

This section reviews drowsiness detection systems and discusses current research activities in this area. To date, a wide range of research and many methods have been proposed to detect drowsiness, which can be grouped into four categories: subjective, vehicle-based, behavioural-based, and physiological-based measurements. Further classification is summarized in Figure 1.1. The following section will review different methodologies, such as Karolinska Sleeping Scale (KSS), with their pros and cons.

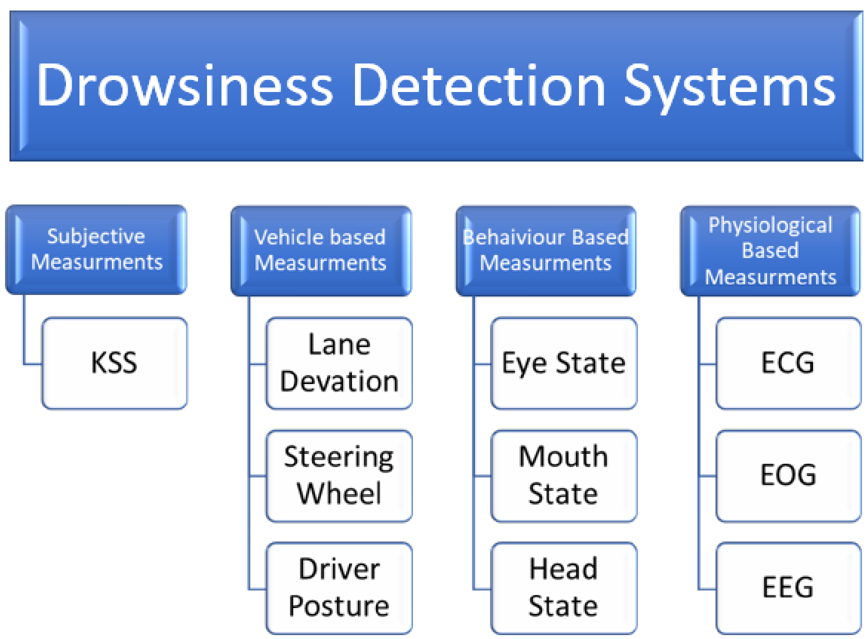

Figure: 1-1. Drowsiness Detection classification and methodologies, subjective, vehicle-based, behavioural-based, and physiological-based measurements.

1.2.1. Subjective Measures

Researchers determine the level of drowsiness by asking human subjects questions verbally or through questionaries. This assessment relies on the individual's experience to evaluate the drowsiness's intensity. Subjective measurement is entirely assessed by individual feedback to alert the person, so it is not considered a real-time assessment tool. The Karolinska Sleeping Scale (KSS) is the most used measure in subjective measurements [12].

1.2.2. Vehicle-based Measurements

This method is based on the driving performance evaluation utilizing the steering wheel and acceleration pedal measurements. These measurements estimate the probability of drowsiness by measuring the deviation from lane position, movement of the steering wheel, and force on the acceleration pedal [13, 14]. In Steering Wheel Movement (SWM), an angle sensor is embedded, and the slight variations in wheel correction are evaluated to find drowsiness [15]. Standard Deviation of Lane Position (SDLP), or the amount that subjects swerve within their driving lane, employs an external camera to track the vehicle swerving from the lanes to assess the driver's drowsiness [18]. In Vehicle-based technology, the path's position may be affected by environmental circumstances and road geometry, which could consequently cause errors in the SWM and SDLP detection software. Furthermore, SWM and SDLP usually happen at the late drowsiness stage when it is too late to avoid an accident. These technologies are unreliable and lose their effectiveness in a real environment [19].

1.2.3. Behaviour-based Measurements

The behaviour-based measurement depends on the driver's concentration level during driving. The first sign of drowsiness is associated with reduced eye blinking and rapid lateral eye movements [2]. This measurement generally is based on the driver's abnormal behaviours, such as eye blinking duration and frequency, yawning, facial expression, and head position [22, 23, 24]. Behaviour monitoring utilizes video cameras and image processing sensors to detect the driver's abnormal behaviours. Environment and driving conditions can affect optical measurements and image processing, so they are not considered reliable [20]. The studies show that using glasses during driving or changing the intensity of light inside or outside the vehicle may dramatically increase the number of false alarms in this method [21].

1.2.4. Physiological-based Measurements

The earlier described drowsiness detection methods have an essential drawback, limiting their usage in practice. All the mentioned techniques can detect drowsiness when the driver starts to sleep, which is often too late to prevent an accident. As a result, they are not considered as early drowsiness prognosis tools. In drowsiness prediction, the time to alert the driver is vital.

The first sign of drowsiness and noticeable alternation appears in the physiological signals like heart rate, respiration rate, blood pressure, and brain signals [25]. Several types of research have been done on electrocardiogram (ECG), electromyogram (EMG), electroencephalogram (EEG) and electrooculogram (EOG) for drowsiness detection [18]. The most noticeable physiological alterations occur in the brain during drowsiness, and EEG signals strongly correlate with drowsiness [11]. EEG signals are considered a reliable and precise drowsiness indicator [11, 25]. Two frequency components of the Electroencephalography signal (Delta and Theta components) increase significantly [25], while heart rate [26], while respiratory rate [27], and blood oxygen concentration [29] decrease in drowsy drivers. Although the other physiological signal-based methods are reliable, the EEG is one of the most predictive and consistent techniques for early drowsiness detection [19].

1.3. Comparison of Current Techniques

In Vehicle-based technology, the position of the path may be affected by environmental conditions and road geometry, which could lead to errors. Behaviour-based drowsiness detection however, is hard to develop robust computer vision algorithms to detect faces and eyes with different colours and weather and lighting conditions [18]. Due to the aforementioned flaws in vehicle and behavior-based techniques, they are considered unreliable for drowsiness detection. Furthermore, they usually detect drowsiness at the late stage when it is too late to avoid an accident. These two methods do not involve drivers in the process; therefore, they are less intrusive. The physiological approach for drowsiness detection is entirely independent of environmental condition changes. One of the problems with this method is collecting biological data, e.g., EEG signals from the drivers, which may not always be feasible. EEG signals are the primary means for the drowsiness level's prognosis, as mentioned in the previous sections. This technique was not feasible for drowsiness detection as it required wet sensors and wires to collect and transfer brain signals. New EEG technology advancements, including dry sensors and wireless technologies like Bluetooth, make drowsiness detection more feasible and affordable during real-world tasks. Although several EEG-based techniques have been proposed for drowsiness detection, several improvements must still be considered and accepted in practice. In the proposed work, with the emergence of dry EEG sensors for detecting brain signals and Bluetooth technology for transferring the EEG data wirelessly, the intention is to develop a sensory system for drowsiness detection. In comparison, EEG-based detection techniques are the most reliable methods for the prognosis of drowsiness nowadays [11, 25].

1.4. Brain Anatomy and Electroencephalography (EEG)

The brain is divided into three main parts: cerebrum, cerebellum, and brainstem, as illustrated in Figure 1.2 [54].

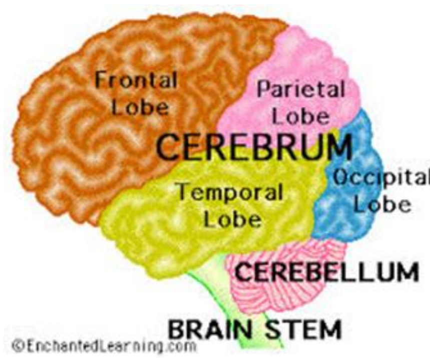

Figure 1-2. Brain Anatomies

The cerebrum is the most substantial and vital portion of the human brain, primarily associated with thoughts, movements, emotions, and motor functions. The cerebrum has two hemispheres: right and left. Each hemisphere is sub-structured into four lobes: frontal, parietal, occipital, and temporal [6]. The frontal lobe handles personality, emotions, problem-solving, motor development, reasoning, planning, parts of speech, and movement. The parietal lobe manages sensation (e.g., pain, touch), sensory comprehension, recognition, the perception of stimuli, orientation, and movement. The occipital lobe controls visual processing, and the temporal lobe deals with identifying auditory stimuli, speech, perception, and memory. The cerebellum is situated at the head's lower back and is responsible for motor control, sensory perception, and coordination. The auto-brain functions, including breathing, consciousness, movements of the eyes and mouth, and the relaying of sensory messages (pain, heat, noise, etc.), heartbeat, blood pressure, and hunger, are controlled by the brainstem that is located at the bottom of the brain and connects the cerebrum to the spinal cord [6].

The nerve cells in the brain are called neurons, and their electrochemical properties enable them to communicate with one another through electrical signals. Electrical activities, which arise from the human brain, are the signatures of neural cell activities and include important complex information about brain function [55]. The brain's electrical activity can be recorded using Electroencephalography (EEG) by placing electrodes on specific locations over the scalp. EEG signals are initiated by summating the synchronous electrical activity of thousands or millions of cortical neurons with similar spatial orientation and spread out to the scalp surface [8]. The EEG signal is broadly utilized to study brain functions.

1.5. EEG Rhythms:

The signals are typically presented in the time domain; however, the frequency is considered one of the most critical measures for assessing clinical EEGs. Usually, the EEG signal amplitude in a healthy adult is between 1 to 100 μV, with a frequency range of 1 Hz to about 100 Hz — with an adequate frequency bandwidth of less than 50 Hz. [8]. The EEG is usually characterized by (1) rhythmic activity and (2) transients. EEG waveforms' rhythmic activities are subdivided into five bandwidths known as alpha, beta, theta, delta, and gamma in clinical practice [55].

Delta (0.5–4 Hz): This waveform is the highest amplitude and lowest in frequency and is seen in adults in slow-wave sleep, known as non-REM sleep (stage 3). This waveform originates in the central cerebrum and is most active in the right parietal lobe of healthy people. The delta frequency source is localized in the thalamus, which is essential in regulating sleep, wakefulness, and consciousness [7].

Theta (4–8 Hz): Theta activity has a frequency range of 4–8 Hz. Theta frequencies increase with increasing emotional stress, mostly frustration or disappointment and occasional task difficulty [9]. Theta frequencies may be seen momentarily during normal wakefulness but become noticeable during drowsiness in adults [8]. Theta activity occurs in healthy infants and children, but high theta activity in awake adults may signal abnormal and pathological conditions [8]. Theta can be recorded from all over the cortex.

Alpha (8–13 Hz): The frequency range between 8 and 13 Hz with an approximate sinusoidal structure is known as alpha activities. Alpha waves are mainly seen in healthy persons, in a non-sleeping relaxation state and with closed eyes [7, 8]. The activities responsible for the Alpha waves are present mainly in the occipital region and reflect sensory, motor, and memory functions. Alpha waves are utilized for meditation and attention level measurements.

Beta (13–30 Hz): Beta band activity indicates 13–30 Hz frequency range. Beta frequencies are more predominant when an individual experiences active thinking, concentration, excitement, or panic instead of normal states. They are generated in the frontal and central portions of the brain [9].

Gamma (>30 Hz): The frequency ranges over 30 Hz are called Gamma activities. These brain activity frequencies are enigmatic, and researchers d where precisely in the brain they originate from and what functionalities they represent. A group of researchers suggests that Gamma waves serve as a carrier frequency for binding various sensory impressions. Simultaneously, some argue that Gamma frequency is a by-product of other neural processes, such as eye movements [9]. The Gamma waves infrequently appear, especially during event-related potential (ERP) tasks and diseases. The gamma waves are most dominant in the front central region of the brain.

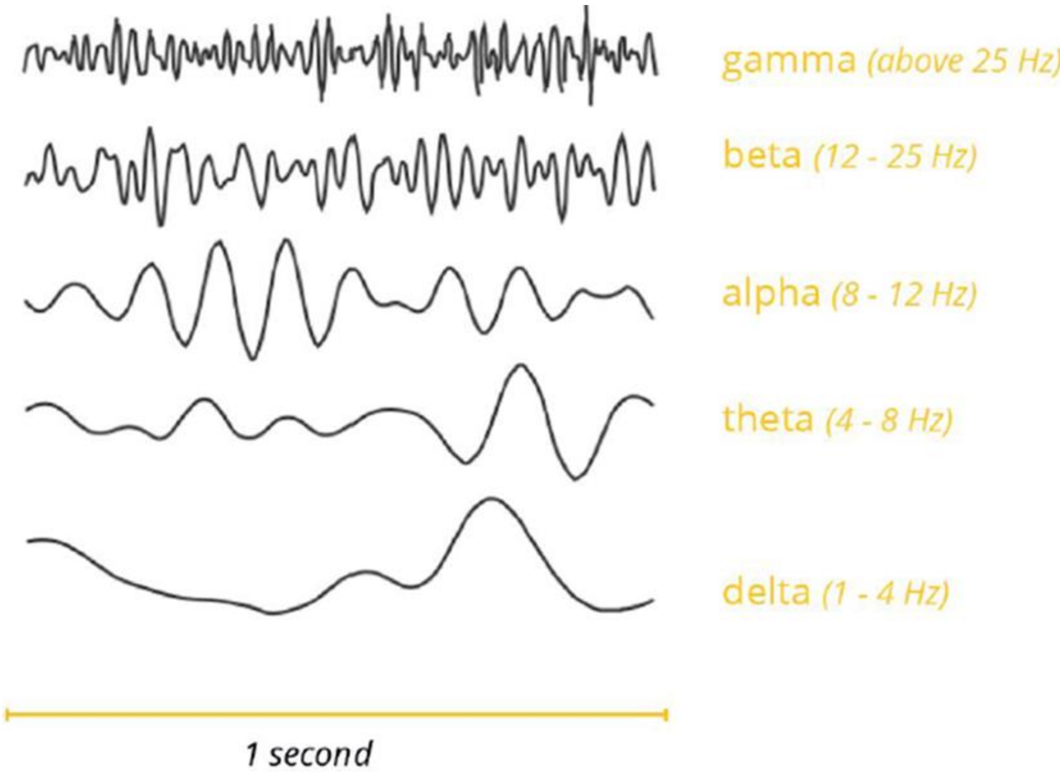

Figure 1-3. Frequency Bands over 1 Second [2]

1.6. EEG Signal Analysis

Despite the efforts of scientists from around the world, the human brain remains the body's greatest mystery. Several experimental techniques have been developed over the past few decades to gain insight into the brain's structure and function: functional magnetic resonance imaging (fMRI), positron emission tomography (PET), near-infrared spectroscopy (NIRS), electroencephalography (EEG), magnetoencephalography (MEG), etc. EEG and MEG are the only neuroimaging techniques that directly and non-invasively record the synchronous oscillations of pyramidal neurons in the cortex [16]. The EEG signals represent brain rhythms and move from the source to the electrodes without delay, known as real-time signals. The EEG signals represent the brain's dynamic, pathological states or psychiatric disorders. Many advanced signal-processing algorithms have been used to analyze brain rhythms. Different relevant features of a specific application could be extracted from the EEG signal through signal-processing methods to diagnose brain disorders. Moreover, brain disorders and diseases like epilepsy, autism, depression, and Alzheimer's could be diagnosed at an early stage by analyzing brain signals [17]. As mentioned earlier, EEG signals contain unique information about brain activities at different brain states, like wakefulness or drowsiness and can be utilized for drowsiness detection [82].

EEG signal processing consists of three stages: pre-processing, feature extraction, and classifying [16]. In general, the raw EEG data is collected by utilizing electrodes on the scalp non-invasively. As the electrodes pick up other sources' electrical activity, extracting useful information from complex EEG waveforms is essential. Brain signal artifacts are signals recorded on the electroencephalogram that is not cerebral in origin and can be divided into physiological and non-physiological [56]. First, the physiological artifacts generated by the patient's body include cardiac, gloss kinetic, muscle, eye movement, respiratory, and pulse artifacts, among many others [56]. The second group is external sources of artifacts like the movement of electrodes or headsets, power lines, swaying, and swinging artifacts. Artifacts should be detected and removed to improve the interpretation of EEG signals.

The first step in brain signal processing is called pre-processing. In the pre-processing stage, all artifacts and noises are removed from raw data to improve the signal-to-noise ratio and facilitate the EEG signal processing.

Measured data is usually not preferred for analysis because of the complexity and the extensive data dimension. The interpretation of those signals is not always straightforward due to their nature or the underlying physiological system that creates the signal. As a result, feature extraction methods have been developed to identify different signal characteristics accurately [106]. The next step in brain signal processing is feature extraction. The essential features are extracted as indices for EEG signal analysis, and data dimension reduction is made in this stage. Classification of brain signals requires an accurate and robust feature detection process in both time and frequency domains [31].

The EEG signal feature extraction methods are generally divided into two main categories: linear (frequency-domain analysis) and nonlinear (time-domain analysis). Linear analysis of EEG signals comprises frequency analysis such as Fourier and Wavelet Transforms and parametric modelling like autoregressive models. Linear algorithms are applied successfully to solve some problems. Fast Fourier Transformation (FFT) and Wavelet Transformation (WT), commonly used for signal analysis, are good choices for stationary signals. However, neurophysiologic processes are often nonstationary and nonlinear by nature [47]. It is widely accepted that the EEG signals are nonstationary and have a nonlinear dynamic [8, 47]. Regardless of the good results associated with the linear analysis in some EEG studies, the EEG signals' analysis loses reliability and accuracy in many cases by ignoring the nonlinear behaviour.

The nonlinear dynamical algorithms using chaos theory have been applied to many areas, including medicine and biology [8]. The EEG signals demonstrate the nervous system's chaotic actions and are increasingly researched to expose features that linear methods cannot measure [6, 34]. Drowsiness generates periodic impacts in EEG signals, affecting chaotic behaviour [34]. Chaotic quantifiers such as the entropy, fractal dimension, and Lyapunov Exponent would be changed due to this effect. These quantifiers could serve as valuable indices for drowsiness prediction and lead to a reliable and accurate prognosis method compared to current technologies.

1.7. Research Objectives

This study utilizes nonlinear data processing using chaos theory to analyze the EEG data for drowsiness prognosis. This study's main objective is to evaluate and identify an appropriate and relevant set of nonlinear features to prognosis drowsiness states from the EEG signals. The final goal of this project was to create a low-cost, minimally-component, reliable, and quick drowsiness prediction system.

The proposed research intends to perform a nonlinear time series analysis on EEG signals for drowsiness prognosis. More specifically, the work presented herein has the following objectives:

- Characterization of alert and drowsy EEG signals using chaotic indicators during the transition from alert to a drowsy state
- Evaluation of a set of chaotic indicators in the prognosis of drowsiness
- Comparison and validation of the performance of the proposed nonlinear approach

- Identification of the classifier inputs to classify EEG signals from the extracted features with a classifier

1.8. Thesis outline

This thesis consists of seven chapters. Chapter 2 consists of dynamical systems and chaos theory and introduces the basic concepts of system dynamics and dynamic system analysis. Chapter 3 studies the feature extraction process using complexity measures in the nonlinear analysis. The concepts of complexity measures, including fraction dimension and entropy, are described in detail. Chapter 4 briefly review the dynamical EEG analysis and quantifiers that measure the chaotic behaviour of EEG signals in different applications, emphasizing drowsiness detection. The experimental setup, data acquisition and methodology are discussed in chapter 5. Chapter 6 presents the result of the chaotic quantifiers in EEG signal analysis during the transition from alert to drowsy state as feature extraction methods, comparing their performances for drowsiness prognosis, and finally, recommending the most suitable method for drowsiness feature extraction based on their performances. Finally, the selected fusion features are applied to a SVM classifier to prognosis the drowsiness and its accuracy investigated in different cases. Based on the achieved experimental results, the proposed model is proven to be in good agreement with theoretical assumptions. Lastly, Chapter 7 provides concluding remarks and recommendations for future research.

Chapter 2.

Dynamical Systems and Chaos theory

This chapter introduces the basic concepts of system dynamics and dynamic system analysis.

2.1. Dynamical System

Dynamics is defined as the systematic study of how things change over time [30]. It is a mathematical model that describes the temporal development of a system. A dynamical system is characterized by its state and dynamics. The states of a dynamical system are variables that fully describe the system's dynamics. A point in m-dimensional space can characterize the state of an m variables system. This space is known as the system's state space (or phase space). Each state is a component in the state-space vector. The state space of a system is valid if all influential variables of the system are known. System dynamics are represented by laws or equations describing how the system's state changes over time. A dynamical system is linear if all the corresponding equations which describe system dynamics are linear otherwise, it is nonlinear [30].

In dynamic system analysis, it is essential to understand what happens in system evolution with time and how the starting conditions influence the system's behaviour [50]. Over time, the following states' sequence defines a curve in the phase-space called trajectory [51]. The trajectory will converge to a state-space subspace at a steady state; this subspace is a geometrical object called the system attractor. Trajectories from all possible initial conditions are attracted to the attractor. Attractors give us an image of the system's dynamic. A sample of attractors and trajectories are shown in Figure 2.1 [57].

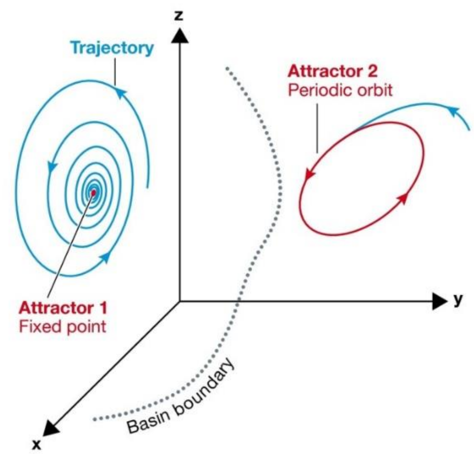

Figure 2.1 Trajectory and Attractor [57]

2.2. Attractor Types and Corresponding Dynamic

According to the resulting geometrical object, attractors can be categorized into four groups [50, 51]:

- Steady-State (Fixed-Point). The attractor converges to a point (steady state) for all the initial conditions unless the system is disturbed from the outside.
- Limit-Cycle. The attractor is a closed one-dimensional curve in the system's state space, representing a periodic motion.
- Limit Torus. Attractor has a complex donut-like form (in an integer dimension). It represents a quasi-periodic motion with a superposition of different periodic dynamics with incommensurable frequencies.
- Strange or Chaotic. Chaos is one type of nonlinear dynamics resulting in complex attractors with fractal geometry. The dynamics corresponding to a strange attractor is deterministic chaos, i.e., the same initial conditions converge to the same final state, but the final state is very different for minor changes to initial conditions [52]. As a result, chaotic dynamics can only be predicted for short periods.

Examples of the four basic types of attractors are shown in Figure 2.2 [52]

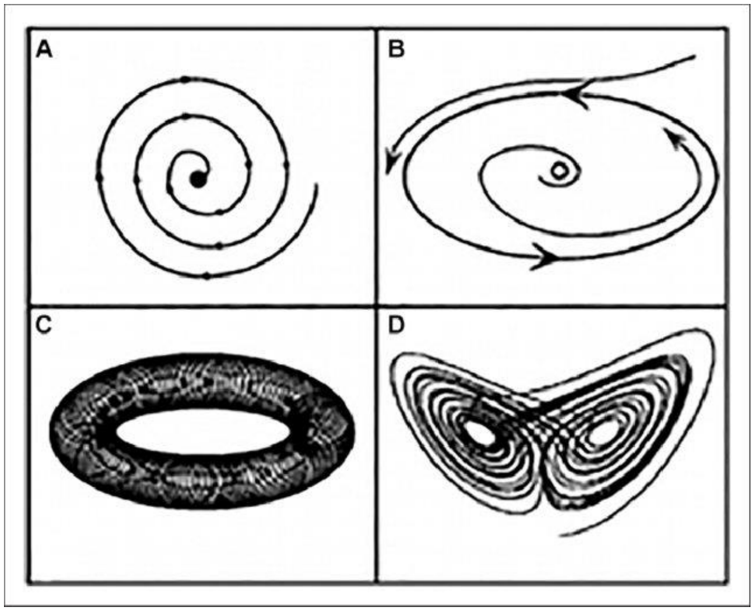

Figure 2.2: Types of Attractors in nonlinear Systems: (A) Steady-State (fixed-point) Attractor, (B) Limit-Cycle Attractor, (C) Limit Torus (or Quasi-periodic) Attractor, and (D) Chaotic (or Strange) Attractor. [52]

To begin, chaos is typically understood as a mathematical property of a dynamical system and a state of disorder [33]. Determinism is the philosophical belief that every event or action is the unavoidable result of previous events and actions, so every event or action may be predicted entirely in advance. If a system is deterministic, the system's future states are predictable. Linear ordinary differential equations usually model deterministic systems. The precise values of state variables at the initial moment and the exact values of systems parameters are needed in such a model.

Most traditional science deals with deterministic and predictable phenomena. In contrast, chaos theory deals with nonlinear systems that are predictable for a while and then appear to become random [42]. Chaos theory embodies three main principles [34]:

- Extreme sensitivity to the initial condition
- Cause and effect are not proportional
- Nonlinearity

Chaos happens when a system has extreme sensitivity to initial conditions. It means two arbitrarily nearby points (states) in such a system will rapidly evolve toward very different positions; in other words, significantly different future trajectories [34]. Edward Lorenz named the sensitivity to initial conditions the "butterfly effect" in his first paper about chaos [42]. Chaotic systems are mathematically deterministic but impossible to predict, and it is more evident in the long-term behaviour than the short-term behaviour of systems. Deterministic chaos is the paradoxical phenomenon of unpredictable behaviour in indeterministic dynamical systems [34]. The main difference between chaos and noise has a root in predictability. Generally, noise is random, structureless, and unpredictable, while chaos naturally encompasses structure and is predictable [34]. Robert L. Devaney formulated a generally used mathematical definition to categorize a dynamical system as chaotic. He says a chaotic system must have the following properties [16]:

- it must be sensitive to initial conditions
- it must be topologically mixed
- it must have dense periodic orbits

2.3. State-Space Reconstruction

Successful reconstruction of the state space will result in an adequate system analysis. The idea of dynamic system modelling is simple and somewhat from a high level. Consider a general differential equation [34]:

$$(dx/dt) = F\,(x,\,t) \qquad (1)$$

In this equation, *x* is a time-series data and function of time, which could be measured. To discover the model, we need to know about *F* and develop a way to figure it out.

Known systems are modelled with some equations. Suppose we do some dynamics of the electromagnetic wave. In that case, we might write down Maxwell's equations, or if we are looking at quantum mechanics, we write those in the Schrodinger equation, so all these scenarios prescribe *F* to discover the system’s dynamic. For a wide range of systems in real life, such as biological systems, the nature of undelaying dynamics is unknown, and it is hard to obtain a set of differential equations at some macro scale for them [34]. Here, the idea is to measure a system and try to back out or infer what governing equations produced that time-series data. It is essential when we cannot measure the system's full state and discover the system model [34]. A dynamic model for these systems can be achieved with a top-down approach, beginning with observing the system's output and working back to state space, attractors, and properties.

Packard et al.[60] brought up a new method of state-space reconstruction in 1980. They presented real-time series modelling in a multidimensional state-space [60]. The method utilized to develop the state-space reconstruction of a dynamic system from the time series is also known as the time series embedding. Therefore, applying nonlinear methods to embed the time series in a phase space with an appropriate dimension is crucial.

The time-delay approach is the most practical procedure for reconstructing the state-space for nonlinear dynamical EEG analysis [34].

Let $\boldsymbol{X_t}$ be an instantaneous measure of the dynamical system, i.e., a sample of the time series obtained by sampling a given system variable [30].

In the time-delay approach, in an *m*-dimensional state-space such as:

$$\boldsymbol{X_t} = \left(x_t, x_{t+\tau}, \ldots, x_{t+(m-1)\tau}\right) \quad (2)$$

The time difference between the state vector x_t's successive components is the lag or delay time, τ and *m* is the embedding dimension. Time-delay embedding begins with a single time series of observations. For reconstructing an *m*-dimensional vector, *m* consecutive values of the time series are taken for the vector's *m* coordinates. This procedure is repeated for the following *m* values of the vectors' time series in the system's state-space. The embedding vectors' sequence forms the system attractor as *t* increases in the state space [44]. The time-delay embedding procedure is shown in Figure 2.3 [52] and Figure 2.4

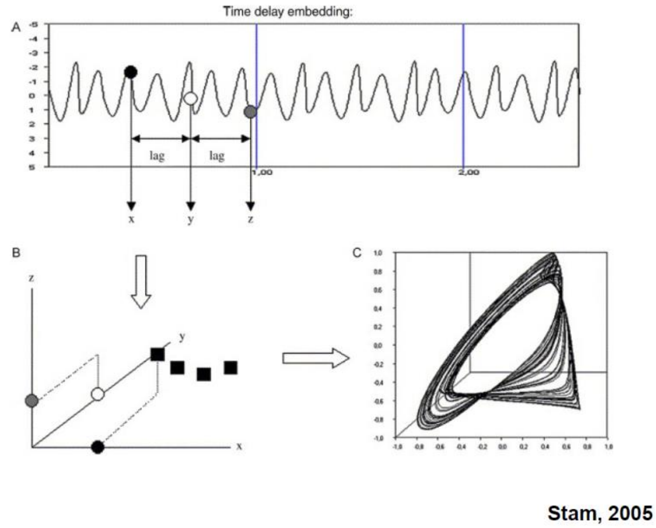

Figure 2.3 Schematic Explanation of Time-Delay Embedding [52]

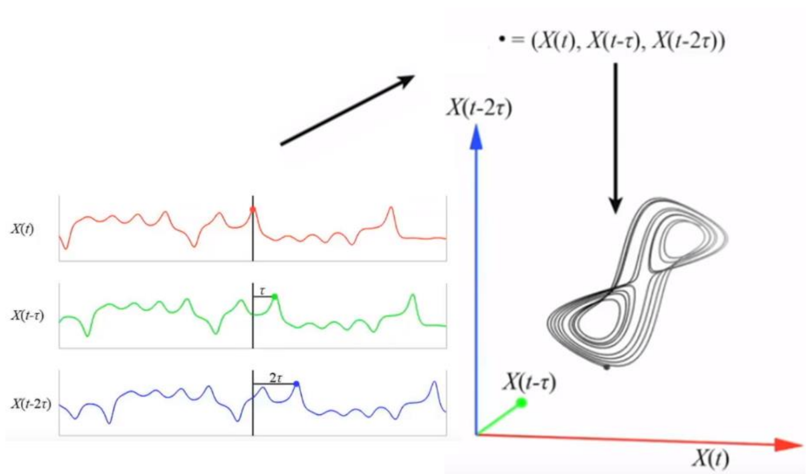

Figure 2.4 Schematic Explanation of Time-Delay Embedding.

The time lag τ, and the embedding dimension, *m*, are the two key parameters, so choosing these parameters is vital for the nonlinear analysis of the EEG waveform [30]. Different choices of *m* and τ yield different reconstructed trajectories. Consequently, wrong choices result in inappropriate outcomes. Fell et al. [45] have proven the significant effect of embedding the time series in a state-space with proper dimension in nonlinear analysis. They proposed the saturation of the correlation dimension method for calculating the precise embedding dimension. This algorithm is utilized by most of the current research in the nonlinear analysis of biosignals.

A practical method is to select τ equal to the time interval. The time series' autocorrelation function (or the mutual information) has dropped to 1/*e* of its initial value [43]. Fraser and Swinney have presented a recursive method of calculating mutual information [80]. They proved that the first minimum in the mutual information provides the best available systematic criterion for choosing time delays for phase portraits [80]. The optimum estimation of *m* is achieved by repeating the correlation dimension analysis for increasing the value of *m* until the result no longer changes [52].

The selection of *m* and τ are interdependent so that the optimum pick τ may depend on the value of *m* and vice versa. The product of τ and (m-τ), called the embedding window, is critical. Taken suggested that τ should be selected so that the highest frequency in the signal can be sampled and *m* in a way that the embedding window equals the wavelength of the lowest frequencies. This method is not any worse than methods that are more sophisticated and use time-consuming algorithms [16].

2.4. Linear Dynamic Analysis

Most linear dynamic analysis methods fall into three main categories: frequency domain, time domain, and time-frequency domain. Frequency domain analysis is a practical method for quantitative signal analysis and is used broadly for linear systems.

Frequency domain analysis also referred to as spectrum analysis, is the practical method of transforming a complex signal into simpler parts in the frequency domain. A complex signal in the time domain is technically described as a sum of many individual frequency components. Spectrum analysis is called a process that quantifies various measurements, such as amplitudes, powers versus frequency, or phase. The most widely used term in frequency analysis is power, which indicates the strength of a specific frequency in the signal. Higher power means that the signal includes a specific frequency to a higher amount. Frequency domain analysis can be applied to the entire signal or a short signal segment. Spectrum analysis is well-suited for periodic signals. The best way to analyze the non-periodic signal is by transforming it into periodic components that fall into Fourier Transform. The Fourier Transform of a signal includes all original signal information in a different form. The Fourier Transform maintains two primary elements of signal amplitude and phase of each frequency component. Discrete Fourier Transform (DFT) is used for discrete signals that run on signal samples and delivers a mathematical estimate of the full integral solution. The DFT is regularly implemented by an efficient algorithm called the Fast Fourier Transform (FFT).

2.4.1. The Definition of the Fourier Transform

The mathematical representation of the Fourier Transform (FT) of a function $f(x)$ is $F(\omega)$. The FT function is defined as:

$$F(\omega) = \int_{-\infty}^{\infty} f(x)e^{-i\omega x}dx \qquad (3)$$

Similarly, the inverse of the FT is defined as:

$$f(x) = \frac{1}{2\pi}\int_{-\infty}^{\infty} F(\omega)e^{i\omega x}d\omega \qquad (4)$$

Where $i = \sqrt{-1}$ and $e^{i\theta} = cos\theta + isin\theta$ (a.k.a. the Euler's formula).

If we consider $f(x)$ as the input data from a signal, the FT function, $F(\omega)$, is the spectrum of the signal (summation of sinusoids). The FT is often expressed in terms of "FT pairs," relating to the frequency domain's time-frequency domain. The general form for FT pairs can be written as $f(x) \leftrightarrow F(\omega)$ or $F\big(f(x)\big) = F(\omega)$.

2.4.2. Discrete Fourier Transform (DFT)

The Discrete Fourier Transform (DFT) is used when we have a discrete and periodic signal. The DFT can be described by using an arbitrary sequence, a_n for values of $n = 0, 1, 2, 3 \dots N - 1$, and $a_n = a_{n+jN}$ for all values of n and j, where N is the period. The general formula for DFT is defined as:

$$A_k = \sum_{n=0}^{N-1} W_N^{kn} a_n \qquad (5)$$

Where $W_N = e^{-i\frac{2\pi}{N}}$ For $k = 0,1,2,3 \dots N - 1$ (the "Nth roots of unity"). These roots of unity are points on the complex unit circle located in the complex plane.

Since each point on the circle is $\frac{2\pi}{N}$ radians apart, a clockwise rotation of an angle can be achieved when multiplying by W_N. A complete rotation or no rotation is 2π radians. Each frequency-domain sequence, A_k, is the Discrete Fourier Transform (DFT) of the time-domain frequency sequence, $a_n$which is made up of N complex numbers. The equation for inverse DFT is:

$$a_n = \frac{1}{N}\sum_{k=0}^{N-1} W_N^{-kn} A_k \quad (6)$$

A significant drawback of Fourier Transforms, in general, is that the analysis is helpful for stationary signals. This means the FT of a signal where the frequencies are the same over time can be correlated to an exact time. However, for a signal where the frequencies are continually changing, such as nonstationary signals like the "chirping" signal, FT will not give information about the specific times when these frequencies occur [4].

2.4.3. The Fast Fourier Transform (FFT) Algorithm

Fast Fourier Transform (FFT) examines how similar the signal is to sine waves consisting of specific pure frequencies. The more similar the signal is to the sine wave, the larger the matching score. For instance, the FFT compares signal data with a 60 Hz sine wave. If the signal data were identical to the sine wave, FFT would return a perfect matching score. FFT analyzes the entire frequency content in a signal. The stronger a specific frequency, the higher the likelihood.

By continuing the analysis of Discrete Fourier Transform using the two-point DFT and the 4-point DFT to 8 points, 16 points, and so on until 2^r points, we arrive at the Fast Fourier Transform (FFT) algorithm for computing the DFT. Computing DFT for any N number of points requires $O * (N^2)$ the number of summations. The DFT is calculated using $O * (NlogN)$ summations when employing the FFT algorithm. The DFT is broken down into $log_2 N$ stages, consisting of $\frac{N}{2}$ butterfly computations.

2.4.4. Quantitative EEG Analysis for Drowsiness Detection

Studies on the EEG signal showed that drowsiness could be detected using the EEG power spectrum [82, 83]. Many researchers concluded that the Alpha and Theta bands' power spectrum analysis is very useful for drowsiness detection. There is a significant increase in the Alpha and Theta power bands when the transition happens from an alert state to a drowsy state. In the alert state, alpha activity is deficient, while in relaxed or drowsy conditions, alpha activity is gradually increased. Different studies have introduced power spectrum analysis of the α, β, β/α, θ/β, (α + β)/θ and (θ + α)/(α + β) of the EEG signal as an indicator for drowsiness prediction. Among these indicators, the (α + β)/θ is the most useful indicator to evaluate drowsiness [83].

2.5. Nonlinear Dynamic Analysis

Nonlinear time series analysis is the best methodology for understanding the dynamics of such systems. The nonlinear dynamic analysis involves two main steps [34]:

- Reconstruction of the dynamics of state space from observations
- Characterization of the resulting attractor through nonlinear dynamic measures

Once these measures have been computed, this information can be used as characteristic features of the analyzed signals in the corresponding application. State space reconstruction of a dynamical system from observations briefly has been explained in section 2.4. The characterization of the resulting attractor and nonlinear measures will be discussed in the next chapter in detail.

Chapter 3. Chaotic Indicators (Complexity measures)

In signal processing, a feature represents a unique property, a detectible quantity, and a functional component gained from a signal segment. The primary purpose of feature extraction is to shrink the data volume and obtain the essential information embedded in the signal. Feature extraction simplifies signal processing by reducing the amount of data while keeping the critical information that accurately describes a vast data set. Employing feature extraction minimizes the complexity of implementation and relives the need to compress the information. The signal feature extraction methods are generally divided into two main categories: linear and nonlinear. The theoretical background of EEG feature extraction analysis based on the dynamical system approach is provided in this chapter.

The next step after reconstructing the corresponding attractor in the state-space is to characterize it using nonlinear indicators. Different measures can be used to characterize attractors and then the system's corresponding dynamics. Different nonlinear indicators characterize reconstructed equivalent attractors' properties and the system's corresponding dynamics in the state-space more precisely [30]. Nonlinear indicators are classified as measures of system complexity and stability. Measuring the complexity of a time series may provide essential insights into the operation of the investigated system.

3.1. Complexity measures:

Complexity measures represent a system's predictability and regularity. A chaotic system possesses two unique characteristics: predictability and regularity. Predictability characterizes the temporal evolution of a dynamical system's states, whereas regularity specifies its trajectory's pattern repetitions. Predictability is the chaotic system's process, while regularity is its output [130]. Two subcategories of predictability approaches exist spatial and temporal dimensionality. Spatial dimensionality needs a reconstruction of the time series state space before evaluating its predictability, while temporal dimensionality characterizes a dynamical system's predictability directly from the signal time series. Correlation dimension and Lyapunov exponents are two main spatial dimensionality measures that will be described in detail later [130]. While spatial dimensionality approaches measure signal complexity by characterizing attractor properties, temporal dimensionality methods interpret time series as a geometric object. Higuchi's fractal dimension (HFD), Petrosian fractal dimension (PFD) and Katz's fractal dimension (KFD) are the three leading temporal dimensionality indices in characterizing nonlinear systems dynamics that estimate FD directly from the time series [130].

Methods that capture a dynamical system's regularity evaluate repetitive time series patterns. Most of these metrics belong to the entropy family of statistics, which measures a system's uncertainty. Regularity indices describe a dynamical system's regularity by approximating the uncertainty of its trajectory inference [130]. Approximate entropy (ApEn), sample entropy (SampEn), FuzzyEn and permutation entropy (PermEn) are the main regularity complexity measures. Costa et al. (2002) presented multiscale entropy to evaluate the multiscale spatiotemporal complexity of physiological signals (MSE). This index is obtained by computing SampEn, FuzzyEn and, PermEn on multiple scales derived from the original signal [131]. Figure 3.1 demonstrate different complexity measures categories.

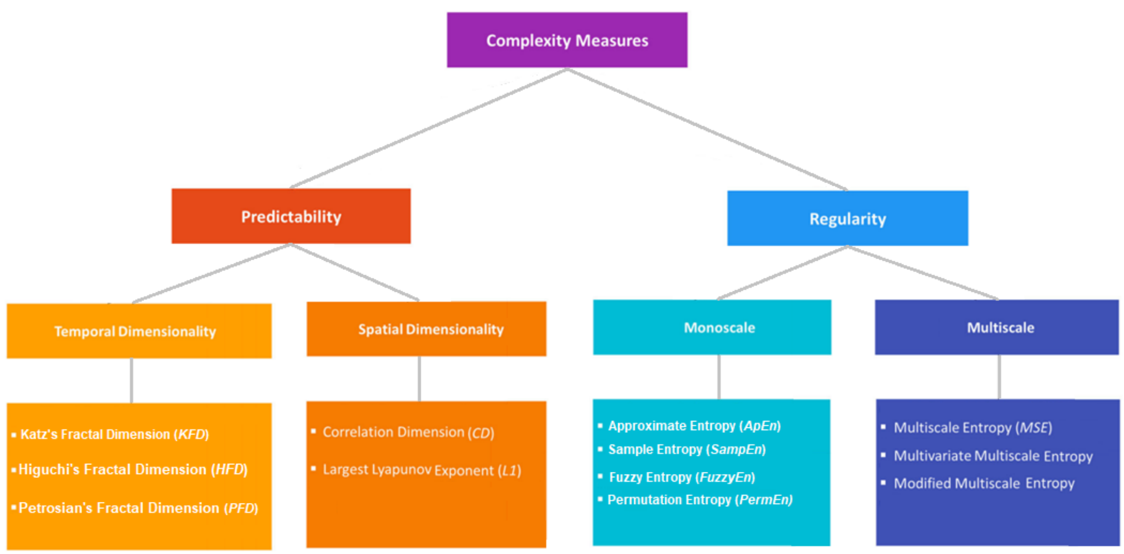

Figure 3-1 Complexity measures categories

Various complexity measurements have been devised to compare time series and discriminate between periodic, chaotic, and random behaviour. These measurements are used on DNA, evolutionary sequences, morphology, development, manufacturing, information systems vulnerability analysis and medical systems [103]. It has been stated that the complexity measure of heart and brain data may discriminate between healthy and ill patients and can even anticipate a heart attack or epileptic episode [104]. Entropies, Fractal dimensions, and Lyapunov exponents are the three main types of complexity parameters. Profound relationships exist between these quantities, all defined for typical dynamical systems. [85]. In the following sections, we address the three most basic complexity measurements.

3.2. Fractal Dimension

A fractal is a mathematical term to describe an object made of several self-similar objects [84]. The magnification of these objects in various scales shows a similar structure. Self-similarity is a typical property of fractals and is a key feature in characterizing them [85]. Self-similarity is categorized into two groups strict self-similarity and statistical self-similarity. Strict self-similarity exists only in artificially generated mathematical objects. The parts of a natural object can be like the whole object on average; therefore, it possesses statical self-similarity [85]. Another feature to characterize the fractals is the fractal dimension. For sets that describe regular geometric shapes, the topological dimension (TD) is used, such as dimension zero for point, dimension one for line, dimension two for the area and dimension three for volume. The theoretical fractal dimension of fractal sets exceeds its topological dimension, and the traditional topological dimension is not suitable for measuring the dimensions of fractals, so the concept of a fractal dimension is employed to characterize fractals [88]. Fractal dimensions can have non-integer values that show a set fills its space qualitatively and quantitatively differently from regular geometric sets. A fractal dimension equal to 1.4 indicates that it fills space more than ordinary lines but less than surfaces. Fractal dimension (FD) is considered an index to characterize the fractal patterns or sets, which quantifies their irregularity or complexity as a ratio of the change in detail to the change in scale [86]. Nowadays, fractal dimensions are utilized in the economy, medicine, biology, physiology, and engineering to characterize systems. The scaling relationships are defined mathematically by the general scaling rule in equation:

$$N = \varepsilon^{-D} \qquad (7)$$

where N is the number of segments, $\boldsymbol{\varepsilon}$ is the scaling factor, and D is the fractal dimension. The value of the D fractal dimension can be found with equation:

$$-D = \frac{\log N}{\log \varepsilon} \qquad (8)$$

The dimension shows the complexity of dynamics (the degrees of freedom), so it is essential in nonlinear time series analysis to estimate the underlying attractor's dimension [16]. The signal fractal dimension computation is a fast and helpful technique for transient detection. The fractal dimension calculating algorithms are applied directly in the time domain, significantly saving the algorithm time-run [87]. Many methods have been proposed for computing the fractal dimension of the attractor. Among them, the following most prominent measures can be highlighted.

3.2.1. Correlation Dimension:

The correlation dimension (D_2) is one of the primary measures for the attractor's fractal dimension and an efficient technique for obtaining experimental data dimension [46]. The correlation dimension usually is a non-integer value larger than one in chaotic systems and reveals the increased complexity of system dimensionality. Grassberger and Procaccia [49] proposed an algorithm to estimate D_2 values of the experimental time series. The idea is to construct a correlation function *C(r)* that measures the probability of pairwise points on the orbit closer together than ***r*** in the state-space. The radial distance around each reference point $\boldsymbol{x}_i$ in the state-space is named ***r***.

$$C(r) = \lim_{N\to\infty} \frac{1}{N(N-1)} \sum_{i=0}^{N-1} \sum_{j=i+1}^{N-1} \theta(r - |x_i - x_j|) \qquad (9)$$

N is the number of data points (the length of the reconstructed attractor) and *Θ* is the Heaviside function. D_2 is calculated using the fundamental definition [30]:

$$D_2 = \lim_{r\to 0} \left(\frac{\log C(r)}{\log(r)}\right) \qquad (10)$$

The vital feature of the Grassberger and Procaccia algorithm is that, for an adequately high embedding dimension *m*, the slope of a linear scaling region of *log (Cr)/log (r)* is an estimate of the correlation dimension D_2 [52]. As mentioned earlier, the maximum estimation (sufficiently high) of *m* can be achieved by repeating the correlation dimension analysis to increase the value of *m* until the result no longer changes. This event is known as saturation of the correlation dimension with increasing the embedding dimension.

3.2.2. Large Lyapunov Exponent (LLE)

The Lyapunov Exponent (λ) measures a system's sensitivity to initial conditions. There are two main varying processes in a chaotic attractor: (i) expansion process, in which the trajectories diverge exponentially fast from similar initial conditions, and (ii) folding process, in which the trajectories will have to turn back into it as time changes [30]. The Lyapunov Exponent determines the exponential divergence or convergence of nearby trajectories in state-space. In other words, it is the average rate of expansion or folding within an attractor [31]. Therefore, λ reflects the system's dynamical behaviour, whereas the attractor dimension indicates its static properties. When a system evolves from a set of initial conditions within radius d_0 in the phase plane, after time t, the trajectories' divergence is characterized by

$$d = d_0 2^{\lambda t} \qquad (11)$$

Lyapunov Exponent λ corresponds to the average rate of the trajectories' divergence. The positive Lyapunov Exponents imply that the system's future state with an unclear initial condition is not predictable and denotes a loss of the system's information. Such a system is also known to be chaotic [32]. When an exponent is negative, the trajectories converge to a common fixpoint. Zero exponent entails that the orbits maintain their relative positions and are on stable attractors [33]. Theoretically, *m* Lyapunov Exponent can be calculated for an *m*-dimensional state-space. The maximum value of λ is called the Largest Lyapunov Exponent (LLE). LLE is of special importance since it identifies chaotic dynamics and periodic signals. Several algorithms have been proposed for calculating LLE [31, 34, 35]. Rosenstein et al. (1993) developed a simple and straightforward approach to estimate the LLE of the reconstructed state without fitting a model to the experimental data [33]. This algorithm calculates the average increase of inter-vector differences starting from pairs of nearest neighbours. It can be defined as the following formula:

$$\lambda_1 = \lim_{t \to 0} \frac{1}{t} \log_2 \frac{l_t}{l_0} \qquad (12)$$

Here λ_1 is the Largest Lyapunov Exponent (bit/Sec), t is a small-time (Sec), l_0 is a small distance between two points on the attractor, and l_t is the distance between the same after a short time t [30]. The two distances are averaged over many pairs of nearest neighbours. This procedure also includes calculating a series of values t so that l_t can be plotted as a function of *t* on a logarithmic plot. Whenever the plot demonstrates a linear scaling area, the slope estimates λ.

3.2.3. Katz's Fractal Dimension (KFD)

Katz's fractal dimension is obtained directly from the time series and defined as [88]:

$$D = \frac{\log(L)}{log(d)} \qquad (13)$$

Where *L* is the total sum of distances between successive points (length of the curve), and *d* is the Euclidean distance between the first point of the sequence and the point of the sequence that provides the furthest distance. Calculating the FD with this formula is dependent on the units of measurement used; therefore, Katz proposed a normalization to resolve this problem as expressed below:

$$FDKatz = \frac{\log(L)}{\log(\frac{d}{a})} = \frac{\log(n)}{\log\left(\frac{d}{L}\right)+\log(n)} \qquad (14)$$

where *a* is the average of the Euclidean distance between successive points of the sample and *n* number of steps in the series *n=L/a* [88].

3.2.4. Higuchi's Fractal Dimension (HFD)

Higuchi's method [91] is a popular time domain technique for identifying the fractal features of complex non-periodic, non-stationary physical data [87, 92]. This technique can precisely determine the time series' fractal dimension. Even in noisy, nonstationary data, it is practical, quick to execute, and can quickly arrive at precise and stable estimates of fractal dimensions [10]. The term "Higuchi fractal dimension" (HFD) refers to the fractal dimension determined using the Higuchi method. The procedure for the method is given below. Consider *x(1), x(2),…, x(N),* the time sequence to be analyzed. Construct k new time series X_k^m defined as:

$$X_k^m = \{x(m), x(m+K), x(m+2k), \ldots, x(m+int[\frac{N-k}{k}].k)\} \qquad (15)$$

for $m=1,2,3,\ldots, k_{max}$

Where *m* indicates the initial time value, *k* indicates the discrete time interval between points (delay), k_{max} is a free parameter, and int represents the integer part of the enclosed value [91]. For each of the curves or time series X_k^m constructed, the average length L_m(k) is computed as:

$$Lm(k) = \frac{\sum_{i=1}^{[\frac{N-m}{k}]} |x(m+ik) - x(m+(i-1)k)|(N-1)}{int[\frac{N-m}{k}].k} \qquad (16)$$

where N is the total length of the data sequence *x* and $\frac{(N-1)}{int[\frac{N-m}{k}].k}$ is a normalization factor. An average length is computed for all time series having the same delay (or scale) *k* as the mean of the *k* lengths $L_m(k)$ for $m=1,2,3,\ldots,k$ $L_1(k), \ldots L_{kmax}(k)$

$$L(k) = \sum L_m(k) \qquad (17)$$

The slope of the best-fitting linear function through the data points $\left\{\left(log\frac{1}{k}, \, log\, L(k)\right)\right\}$ is defined as the Higuchi fractal dimension of the time series *X* [90, 91].

The calculated HFD depends on the length of the time series and is affected by an internal tuning factor K_{max} that plays a crucial role in the estimation of HFD. One drawback of utilizing the Higuchi method is that parameters must be employed, and improper parameter selection results in the erroneous calculation of fractal features [94]. Although the approach has been utilized for decades and is frequently used today, there is no agreement on the best way to identify the optimum k_{max} parameters. Several studies have been conducted to address the issue of proper tuning factor k_{max} selection. Accardo et al. [95] used the Higuchi method in their research of electroencephalograms and found the best pair of electrodes (k_{max}, *N*). They tested with k_{max} = 3-10 on time series with lengths ranging from *N* = 50 to 1000 and determined that k_{max} = 6 was the best value [95].

3.2.5. Petrosian's Fractal Dimension (PFD)

A fast algorithm to calculate the fractal dimension of a signal was introduced by Petrosian. This estimation is the fractal dimension of a binary sequence originally defined by Katz [88]. Signals are usually analog and should be translated into binary series. There are four main algorithms to derive this binary sequence. The most practical method is called the Petrosian D algorithm [95]. First, the consecutive samples in the time series are subtracted. Next, the binary sequence is formed by assigning a '1' for every difference that exceeds a standard deviation magnitude, and a '0' is given otherwise. The FD is then computed as [95]:

$$D = \frac{\log_{10} n}{\log_{10} n + \log_{10}(\frac{n}{n+0.4N\Delta})} \qquad (18)$$

where *n* is the length of the sequence (number of points), and NΔ is the number of sign changes in the generated binary sequence.

3.3. Entropy

Entropy analysis has gotten much attention among the vast number of nonlinear dynamical methods in recent decades. It evaluates the complexity, or irregularity, of time series. Many studies have proven its wide suitability in time series of limited length, short length, or even concise length [96].

Entropy came from a discipline called thermodynamics, a branch of physics. It was initially proposed as a state function of a thermodynamic system that depends only on the current state while independent of how the state is obtained. It was later found that this macroscopic concept meant uncertainty or irregularity that microscopically measures the probable number of microscopic states in which the system can be arranged [97].

As a measure of disorder or uncertainty in the data, information entropy was first introduced by Shannon in 1949 [75]. Entropy is the diminishing rate of the necessary information for future state estimation, expressed in bits per second. Generally, an attractor's information loss rate states its entropy [34]. In information theory, the information source's uncertainty and the probability distribution of the draw samples are measured by entropy [76]. Since entropy states uncertainty, it can indicate the level of chaos in the system. A higher entropy measure denotes more uncertainty and a higher chaotic system [16].

In the field of time series analysis, this concept sparked the idea of evaluating the unpredictability of the evolution of dynamic systems, especially the Kolmogorov entropy of time series (or Kolmogorov-Sinai entropy, a special case of Kolmogorov entropy with time lag being equal to unity) [107]. The Kolmogorov-Sinai entropy algorithm was sensitive to noise, making it impossible for real-world applications. An approximate entropy algorithm with reasonable robustness to noise and relatively stable for medium-time series was proposed by Pinkus in 1991[113]. However, this method had unreliable performance in short-length data and strong dependence on input parameters, so investigators proposed other methods to improve its performance. Entropy analysis has been attracting increasing attention in the recent two or three decades. Many different entropy methods have been introduced to quantify the signal's complexity with various applications to date. Shannon entropy, Maximum entropy, Renyi's entropy [42], Kolmogorov Sinai entropy [38], Approximate entropy [39], Sample entropy [41], Fuzzy entropy, and Permutation entropy are some of the entropy algorithms in chronological order. These estimators are categorized as Embedding entropies. Embedding entropies measure the uncertainty of the signal directly in the time series to estimate the entropy. Spectral entropy [40] assesses the energy distribution and utilizes the signal's power spectrum's amplitude components as the probabilities in entropy calculations [58].

In the following subsections, important and practical entropy measurements, including Approximate Entropy (ApEn), Sample Entropy (SampEn), Fuzzy Entropy (FuzzyEn), and Permutation entropy (PermEn), will be briefly introduced.

3.3.1 Approximate entropy (ApEn)

Approximate entropy (ApEn) is a well-known measurement for chaos and quantifies the system's complexity, irregularity, and unpredictability. Pincus introduced it as an indicator of system complexity to assess the time series’ irregularity without previous knowledge about the data source [39]. It is defined as the logarithmic likelihood that calculates how the close data sets' patterns will remain closed for the following comparison with a longer pattern [73]. A time series with many repetitive patterns has a low ApEn; a process with fewer predictable patterns has a higher ApEn. The minimum value for ApEn is 0, suggesting an entirely predictable sequence. A high value of ApEn indicates random and unpredictable variation, whereas a low value of ApEn indicates regularity and predictability in a time series. ApEn has been used to characterize the degree of randomness in the physiologic time series [39]. ApEn is less sensitive to noise, useful in short-length data calculations, and resistant to short, strong transient interferences like spikes [81]. These prominent features make ApEn attractive for use in physiological signal processing. ApEn's application is spreading rapidly, especially for real-time applications [81].

For a time-series of N points $u= u(i)$, $1 \le i \le N$, its *m*-dimension state space representation

$$x_m(i) = \{u(i), u(i+\tau), \dots, u(i+(m-1)\tau)\} \quad (19)$$

where $1 \le i \le N - m\tau$ and τ is the time delay parameter, which, together with the dimension parameter *m*, determines how well the state space reconstruction of the dynamical system is. To quantify whether two vectors, namely, $x_m(i)$ and $x_m(j)$, are similar, the Chebyshev distance between the two vectors is calculated as follows:

$$d[x_m(i), x_m(j)] = \max_{0 \le k \le m-1} (|u(i+k) - u(j+k)|) \quad (20)$$

In ApEn, the percentage of the vectors $x_m(j)$ that are within *r* of $x_m(i)$ is calculated by the $C_i^{(m)}(r) = \frac{N_i^{(m)}(r)}{N-m\tau}$ where $N_i^m(r)$ indicates the number of *j*'s that meet $d_{i,j} \le r$, and $1 \le j \le N - m\tau$. And then, the average of the percentage over $1 \le i \le N - m\tau$ after the logarithmic transform is defined by

$$\varphi^m(r) = \frac{1}{N-m\tau} \sum_{i=1}^{N-m\tau} \log C_i^{(m)}(r) \quad (21)$$

Similarly, $\varphi^{(m+1)}(r)$ is defined after increasing the dimension to *m + 1*. Then, the ApEn value of the time-series **u** can be calculated by [84]:

$$ApEn(m, \tau, r) = \varphi^m(r) - \varphi^{(m+1)}(r) \quad (22)$$

Two parameters, *r*, and *m* must be specified before the ApEn calculation. *m* is the vector's embedding dimension to be formed, and *r* is the affective filter (a threshold), which typically has values pegged to the standard deviation of the sequence. Usually, r = 20% of the standard deviation of the amplitude values and m = 2 [98]. $C^m(r)$ is a correlation integral that should be calculated in the following equation.

3.3.2. Sample Entropy (SampEn)

Dependent on record length is one of the ApEn method's drawbacks and is usually lower than predicted for short records. Another disadvantage of ApEn is its inconsistency [98]. To address the shortcomings of ApEn, sample entropy (SampEn) was offered as a replacement for ApEn by omitting self-matches, improving computation time by half in contrast to ApEn. SampEn has the benefit of being consistent and essentially independent of record length [98].

For a time series of *N* points **u** = u(i), 1 ≤ i ≤ N, its *m*-dimension state space representation

$$x_m(i) = \{u(i), u(i+\tau), \ldots, u(i+(m-1)\tau)\} \qquad (23)$$

where $1 \le i \le N - m\tau$ and τ is the time delay parameter, which, together with the dimension parameter *m*, determines how well the state space reconstruction of the dynamical system is. In SampEn, self-matches are excluded when calculating the percentage of the vectors $x_m(j)$ that are within *r* of $x_m(i)$,

by $A_i^{(m)}(r) = \frac{N_i^{(m)}(r)}{N-m\tau-1}$ where $N_i^m(r)$ indicates the number of *j*'s that meet $d_{i,j} \le r$, and $1 \le j \le N - m\tau,\ j \ne i$. The average the percentage $A_i^{(m)}(r)$ over $1 \le i \le N - m\tau$ is defined by:

$$\varphi^m(r) = \frac{1}{N-m\tau}\sum_{i=1}^{N-m\tau} \log A_i^{(m)}(r) \qquad (24)$$

Similarly, $\varphi^{(m+1)}(r)$ is defined after increasing the dimension to *m + 1*. The probability that the two sub-sequences match for *m* points and the probability of a match for *m+1* points, where *r* is the tolerance for accepting matches, give the sample entropy, defined as the average over multiple templates of the log ratio of A/B [99]. Then, the SampEn value of the time-series **u** can be calculated by [98]:

$$SampEn(m, \tau, r) = \ln \frac{\varphi^{(m)}(r)}{\varphi^{(m+1)}(r)} \qquad (25)$$

Parameters *m* and *r* must be defined according to criteria of error, signal properties and expected entropy values and are dependent on the properties of the signal under exam [99]. Sample entropy is independent of the recording length and displays relative consistency under various conditions.

3.3.3 Fuzzy Entropy (FuzzyEn)

ApEn and SampEn both utilize a Heaviside function to compare the similarity of vectors, a two-state binary classifier in which vectors are either close or not close. However, this may not accurately capture the borders between classes, particularly in biological data, where the distinctions between classes may be fuzzy. FuzzyEn was proposed to overcome this issue using a fuzzy function instead of the Heaviside function to calculate the similarity degree between vectors [13]. FuzzyEn has been used to evaluate various types of biomedical data since its inception, including electromyograms, EEGs, gait, and heart rate variability [101]. Comparative studies show that the FuzzyEn method results surpass the ApEn and SampEn. In addition, new research reveals that FuzzyEn is a robust entropy estimator when missing samples are present in the biomedical signals being analyzed [101].

Given *N* data points from a time series *{x(n)} = x(1), x(2), . . . , x(N)*, FuzzyEn can be calculated using the following algorithm [100]:

For *1 ≤ i ≤ N - m + 1*, form *m*-vectors $x_m(1)\ldots x_m(N-m+1)$ defined as:

$$x_m(i) = \{x(i), x(i+1), \ldots, x\big(i+(m-1)\big)\} - x_0(i) \qquad (26)$$

These vectors represent *m* consecutive *x* values, commencing with the *i*th point, with the baseline $(xo(i) = \frac{1}{m}\sum_{j=0}^{m-1} x(i+j))$ removed.

Define the distance between vectors $x_m(i)$and $x_m(j)$, $d_{ij,m}$, as the maximum absolute difference between their scalar components. Given *n* and *r*, calculate the similarity degree $d_{ij,m}$ of the vectors $x_m(i)$and $x_m(j)$ with a fuzzy function:

$$D_{ij,m} = \exp\left(\frac{-\left(d_{ij,m}\right)^n}{r}\right) \qquad (27)$$

Define the function $\varphi_m$as:

$$\varphi_m(n,r) = \frac{1}{N-m}\sum_{i=1}^{N-m}\left(\frac{1}{N-m-1}\sum_{i=1,j\neq i}^{N-m} D_{ij,m}\right) \qquad (28)$$

We increase the dimension to *m + 1*, form vectors $x_{m+1}(i)$ and, subsequently, obtain the function φ_{m+1}

For time series with a finite number of samples *N*, FuzzyEn can be estimated with the following equation [100]:

$$FuzzyEn(m,n,r,N) = ln\varphi_m(n,r) - ln\varphi_{m+1}(n,r) \qquad (29)$$

3.3.4 Permutation entropy (PermEn)

Permutation entropy (PermEn) is a reliable time series tool that quantifies the complexity of a dynamic system by capturing the order relations between values in a time series and extracting a probability distribution of the ordinal patterns [110]. It defines a permutation vector π by indexing its elements in ascending order for every signal motif of length *m*. Then, the frequency of each permutation pattern π_j ($1 \leq j \leq m!$) is computed, and the PermEn of the original time series is defined by the Shannon entropy of permutation patterns [110].

The permutation entropy of a signal x is defined as:

$$H = -\sum_{i=0}^{m!} p_i(\pi)\log_2 p_i(\pi) \qquad (30)$$

where the sum runs over all *m*! permutations π of order *m*. This is the information contained in comparing *m* consecutive values of the time series. It is clear that $0 \leq H(m) \leq \log_2(m!)$ where the lower bound is attained for an increasing or decreasing sequence of values, and the upper bound for a completely random system where all *n*! possible permutations appear with the same probability. The embedded matrix Y is created by:

$$y(i) = [x_i, x_{i+\tau}, \dots, x_{i+(m-1)\tau}] \qquad (31)$$

$$Y = [y(1), y(2), \dots, y\big(N-(m-1)\big)\tau]^T \qquad (32)$$

τ is the embedding time delay, and m is the embedding dimension. The maximum value of *H*(*m*) can be obtained as $\log_2 m!$ when all the symbol sequences have the same probability distribution as P_l=1/*m*!. Therefore, the permutation entropy of order *m* can be normalized as:

$$PermEn_{m,norm} = \frac{1}{\log_2 m!} \sum_{i=0}^{m!} p_i(\pi)\, log_2\, p_i(\pi) \qquad (33)$$

Among its main features, the PermEn approach [110]:

- It is non-parametric and is free of restrictive parametric model assumptions.
- It is robust with noise, computationally efficient, flexible, and invariant with nonlinear monotonic transformations of the data.
- Relies on the notions of entropy and symbolic dynamics.
- Accounts for the temporal ordering structure (time causality) of a given time series of real values.
- Allows the user to unlock the complex dynamic content of nonlinear time series.

Chapter 4. Literature review - Nonlinear Dynamical EEG Analysis and Support Vector Machine (SVM)

This chapter will briefly review the dynamical EEG analysis in different applications, emphasizing drowsiness detection.

Most physiological knowledge is based on linear system theory. It is a contemporary challenge to identify characteristics from physiological signals or time series. Attempts have been made to mine the data using frequency-domain and time-frequency analysis. However, the outcomes of these conventional procedures have not been entirely satisfying [96]. One explanation might be that those that these methods could catch are generally also visually recognizable, which is not the case with physiological data. The important physiological or illness aspects may be hidden below signal oscillations.

Researchers from interdisciplinary fields have proposed the concept of nonlinear dynamical analysis in recent decades. Chaotic behaviour is perceived in many dynamic biological systems, and there is strong empirical evidence of chaotic behaviour at every level of biological organization, including the nervous system [89]. Grassberger and Procaccia's algorithm facilitated applying the element of chaos theory to various observations. The nonlinear time series analysis introduced a new landmark and established a new interdisciplinary field of nonlinear brain dynamics. The nonlinear methods are the best tool to analyze the processes within the nervous system, regardless of whether they are ion channel activity, neuronal, population, or network activity [89]. Biomedical signals such as EEG are naturally short, non-linear, and noisy, resulting from traditional signal processing methods (linear time series analysis) that can be skewed by noise and not promising [59, 64]. The early years of nonlinear analysis of the brain were roughly between 1985 and 1990. The first study of nonlinear EEG analysis of neural activity was done in 1985 by Rapp et al. Simultaneously, Babloyantz et al. reported chaotic dynamics of brain activity during the sleep cycle [60]. Over the past 20 years, many studies have looked at chaos in brain signals [63].

Fractal geometry is a prominent feature of deterministic chaos. In chaotic systems, a subset of the phase space known as a strange attractor possesses a fractal structure characterized by self-similarity and non-integer dimension. The fractal dimension of a signal represents a powerful tool for transient detection. This feature is used to identify and distinguish physiologic states in electroencephalograms and frequently is used in EEG signal processing for different applications. A variety of algorithms are available for the computation of fractal dimensions.

Among the various nonlinear analysis methods, entropy algorithms have a variety of applications in biomedical signal processing [3]. Many different entropy algorithms have been introduced in the literature over the years, and all rely on detecting chaotic or regular behaviour in biomedical signals. Entropy methods have shown great promise in analyzing electroencephalogram (EEG) signals. This is mainly caused by the high complexity of the human brain and the nonlinear interactions between neurons, which results in the EEG signal whose dynamics can be characterized in better detail using entropy algorithms.

The EEG signal is affected by numerous events, including epilepsy, Alzheimer, coma/anesthesia, depression, schizophrenia, meditation, fatigue, sleep, and drowsiness. Much research has been conducted to characterize EEG signals in these events during the last decade. Reviewing the results of this research allows us to understand better methods that pave the way for the proper use of complexity measures in early drowsiness diagnosis. The following sections will describe the effects of some of the main events on the EEG signal and the outcomes of nonlinear EEG signal analysis in these events.

4.1.1. Epilepsy and Seizure detection

Epilepsy is a brain disorder where normal neuronal activity gets affected and is one of the most important applications for nonlinear EEG analysis. Babloyantz and Destexhe were the first to study the nonlinear seizure analysis [52]. They reported that the correlation dimension of this seizure was substantially lower than the dimension of a normal EEG. Iasemidis et al. and Swiderski et al. found that the Largest Lyapunov Exponent during epileptic seizures decreases and can be used for predicting seizures [52,37]. Several studies for nonlinear seizure prediction were proposed, involving Studies on Approximate entropy (ApEn) [112,113,114,115], Permutation entropy (PermEn) [N106,107,108,109,110], Sample entropy (SampEn) [118,122], and Fuzzy entropy (FuzzyEn) [122,123] provide evidence that absence of epilepsy can be effectively distinguished.

4.1.2. Alzheimer

Jeong et al. further utilized nonlinear parameters to identify brain disorders such as Alzheimer's [77]. They measured the correlation dimension and the first positive Lyapunov exponent of the EEGs in patients and healthy control subjects. They showed that Alzheimer's patient's EEG has a significantly lower correlation dimension and the first positive Lyapunov Exponent than the healthy control subjects [32]. Most studies show that Alzheimer’s disease (AD) is typically associated with a loss of EEG complexity. Fan et al. (2018) and Yang et al. (2013) reported that multi-scale entropy (MSE) is sensitive to the severity of AD symptoms [125,126]. Their research proved that entropy significantly declined from moderate to severe AD stages. Samantha Simons et al. (2018) utilized fuzzy entropy to analyze the AD patient's EEG signals, and they found that AD patients had significantly lower FuzzyEn values than control subjects [124].

4.1.3. Anesthesia

Another application of entropy measures is monitoring the depth of anesthesia. Watt and Hameroff (1988) were the first to propose the utility of nonlinear EEG analysis as a tool for measuring anesthetic depth [120]. Widman et al. (2000) discovered a relationship between the correlation dimension and the estimated sevoflurane concentration in the brain [122]. Van den Broek's doctoral dissertation (2003) confirmed the correlational dimension's usefulness as an estimate of anesthetic depth [123].

Rezek et al. (2004) successfully demonstrated the practicality of entropy measures for characterizing the various phenomenon from the EEG signals by applying stochastic complexity features on EEG signals during periods of anesthesia [35]. Liang et al. (2015) compared twelve entropy indices, including approximate entropy (ApEn), sample entropy (SampEn), Fuzzy entropy, and permutation entropy (PE) measures in monitoring the depth of anesthesia. They found that permutation entropy performed best in tracking EEG changes associated with different anesthetic states and that approximate entropy and sample entropy performed best in detecting burst suppression [116].

4.1.4. Sleep

As mentioned earlier, the first study on nonlinear analysis of the human EEG was done with sleep recordings data, which was done by Babloyantz et al. in 1985 [72]. This study concluded that the more profound the sleep, the lower the brain dynamics complexity, and the dimension is the smallest [60]. Since that time, sleep has become significant research focused on nonlinear dynamics. Many researchers have focused on measuring the correlation dimension and the Largest Lyapunov Exponent during the different sleep stages.

In the fundamental nonlinear analysis of healthy adults' sleep EEG signals, the correlation dimension (D_2) has been consistently reported to decrease from wake to sleep in different stages and increase during rapid eye movement sleep (REM) [66, 67, 70, 71, 72, 73, 74].

Fell et al. studied 15 normal subject EEG in the sleep stages one to five and measured the Largest Lyapunov Exponent during the different sleep stages in 1993 [68]. They found statistically significant differences between the values of the Lyapunov Exponent for different sleep stages. The overall outline of these studies is that deeper sleep stages are always linked with a lower complexity as represented by lower

Shannon entropy, permutation entropy, spectrum entropy, approximate entropy (ApEn), sample entropy (SampEn), and multiscale entropy (MSE) are some of the entropy analyses that have been studied in sleep EEG signals [16]. ApEn, SampEn, and MSE are the three main methods commonly used for EEG entropy analyses. Regardless of the different entropic methods, all the study results are consistent and report that the entropy of sleep EEG signals declines from wake-to-sleep stages one to three and rises during REM for healthy adults [76]. Figure 4.1 demonstrates reported trends of fractal-based and entropy-based outcomes for different sleep stages.

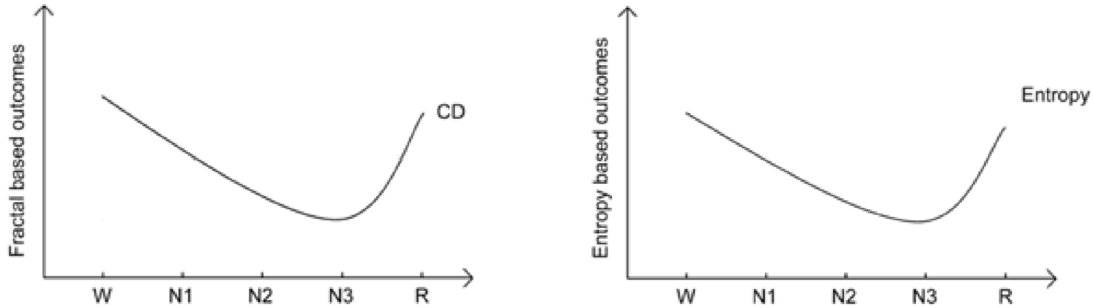

Figure 4-1: Reported Trends of Fractal- and Entropy-based Outcomes for Different Sleep Stages [76]

4.1.5. Drowsiness

This section examines the work done on drowsiness detection, with a particular emphasis on the used features.

Belakhdar et al. [140] employed spectral analysis (FFT) on the α band with an ANN classifier and achieved an average accuracy of approximately 88.80%. Correa et al. [141] used frequency and time-frequency domains, including FFT and DWT, for feature extraction with ANN classifiers and achieved an 83.6% drowsiness detection accuracy rate. Chen et al. [142] achieved 76% accuracy in drowsiness detection using γ, γ/α, θ, θ/γ, $\gamma/(\alpha+\beta+\gamma)$, and γ/θ EEG features with Karolinska Sleepiness Scale (KSS) as the ground truth and SVM classifier. Hu et al. [143] employed α, β, γ, and frequency domain statistics in addition to EOG signal characteristics. Using binary ground truth labels, the authors could detect drowsiness with an accuracy of 75%. Picot et al. [144] utilized α, β, and power spectrum features along with an EOG signal with three levels of ground truth data that were labelled by experts and achieved an accuracy of 80.6%. Liu et al. [145] applied ApEn and Kolmogorov entropy of the α, β, γ, and θ frequency bands with the KSS Stanford sleepiness scale for labelling the ground truth data, and 84% accuracy has been achieved with a hidden Markov model classification. Chaudhuri and Routray [146] employed just three ApEn, SampEn, and modified SampEn entropies as features for fatigue detection. Their experiment was labelled into seven fatigue states. Utilizing SVM, they achieved 86% accuracy. Zou et al. [147] used the multiscale PE, multiscale SampEn, and multiscale FuzzyEn with ground truth labels based on Li's subjective fatigue scale. The accuracy achieved was 88.74%.

Mardani and colleagues have measured Higuchi's and Petrosian's fractal dimensions of the EEG signal, and they reported that the extracted features could discriminate between alertness and drowsiness. It is prominent in most EEG channels [75]. Figure 4.2 shows extracted features, Higuchi, and Petrosian fractal dimensions of the EEG signal for trials in alertness and drowsiness level [75]. They achieved an accuracy rate of drowsiness detection of about 83.3% using an ANN classifier.

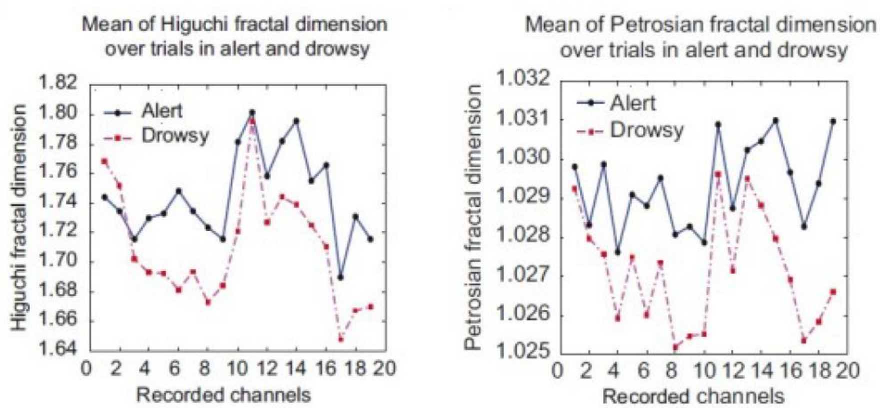

Figure 4-2: Mean of Higuchi and Petrosian Fractal Dimensions of EEG Signal for Trials in Alertness and Drowsiness Level [75]

Min et al. [127], Hu et al. [138], and Zhang et al. [129] used ApEn, and SampEn for fatigue detection, and the results were promising.

In conclusion, many publications have conducted sleep studies analyzing the EEG with characterizing measures. In particular, the authors have studied sleep stages and normal and pathological conditions. Despite much research on sleep stages and fatigue, a few studies have been done on drowsiness EEG signal analysis with nonlinear techniques. The complexity measure changes of EEG signal during the transition from alert to the drowsy state are unknown. Their ability to distinguish between alertness and drowsiness has yet to be studied.

In this research, the compelling goal is to bring state-of-the-art technologies to mining trucks for rapid and accurate prediction and drowsiness monitoring. According to the literature review and researched EEG signals, chaotic indicators are efficient tools for analyzing EEG signals in different applications. This study evaluates the usability and effectiveness of the chaotic quantifiers of EEG signals to develop an early drowsiness prognosis system, including predictability and regularity indices on drowsiness prognosis. The potential of forecasting drowsiness is explored and attempted in this work by dynamically reconstructing the EEG signals and assessing them by a set of nonlinear features. Furthermore, this study makes an effort to analyze EEG signals with nonlinear methods and evaluate the drowsiness states. This research studies the different techniques of applying nonlinear time series analysis methods for EEG signals to prove that concepts initiated from the theory of nonlinear dynamics can characterize the drowsiness and appropriateness for drowsiness prognosis. Compared with a single index, the fusion of indices is a better way to achieve complementarity among different signal features and obtains a more comprehensive expression of the signal.

4.2. Classifiers- Support Vector Machines

The main objective of this study is to develop an intelligent, reliable, and effective drowsiness prognosis system. So far, the nonlinear feature extraction methods of EEG signals are discussed in the previous section. The last step to developing an intelligent system is applying these indices to classifiers. Then, the classifiers use the extracted features as inputs. In this work, we propose to use support vector machine classifiers. The theory of these classifiers is discussed in this section.

Support vector machines (SVM) are supervised learning models with algorithms that analyze data and identify patterns [133]. SVM is a helpful tool for classification problems. An SVM training algorithm builds a model that shows the training samples as points in space from a set of training samples belonging to one of two groups. The points are mapped so that the samples from the two categories are split by an optimal hyperplane, creating the largest gap possible between samples from the distinct categories. A new set of samples can then be mapped to the same space and classified based on which side of the hyperplane they lie.

4.2.1. Linear SVM

Given a set of training data D, a set of n points of the form

$$D = \{(x_i, c_i)|x_i \in R^p, c_i \in \{-1, 1\}\}_{i=1}^{n} \qquad (34)$$

where each x_i is a P-dimensional real number or vector and c_i is the label indicating the class to which the point x_i belongs. The goal is to find the maximum margin hyperplane that divides the points with $c_i = -1$ from those with $c_i = 1$ [133]. A hyperplane can be written as the set of points x satisfying $w.x - b = 0$

where · denotes the dot product. w is a surface normal vector perpendicular to the hyperplane. The offset of the hyperplane from the origin along w is given by

$$\frac{b}{\|w\|} \qquad (35)$$

To maximize the margin between the parallel hyperplanes separating the two classes of data, w and b are chosen such that $w.x_i - b = -1$ and $w.x_i - b = 1$

For linearly separable data, the two hyperplanes can be chosen so that no points lie between them, and then the distance between them can be maximized [135]. The distance between the two hyperplanes is given by $\frac{2}{\|w\|}$ so the term to minimize is $\|w\|$. To prevent data points from falling into the margin, a constraint is added such that $w.x_i - b \leq -1$ or $w.x_i - b \geq 1$ for x_i of the two classes. These can be rewritten as

$$c_i(w.x_i - b) \geq 1, 1 \leq i \leq n$$

The SVM training optimization problem is therefore given by

$$min_{w,b}\|w\| \qquad (36)$$

subject to $c_i(w.x_i - b) \geq 1$

See Figure 3.2 for a graphical example of SVM training.

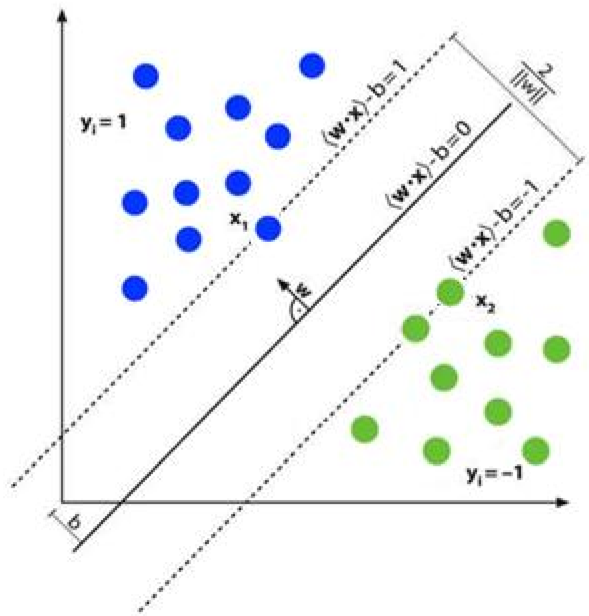

Figure 4-3 SVM training to find the optimal hyperplane (solid black line) separates the samples from two classes (orange and blue circles) with maximum margin. Circles represent support vectors with outlines

4.2.2. Soft margin SVM

In cases where no hyperplane can separate the data points from the two categories, a soft margin approach can be used to create a hyperplane that splits the points as effectively as possible while maximizing the distance to the nearest adequately split data points. [134]. The slack variables ε_i are introduced, which measure the degree of misclassification of each x_i. Equation 8 then becomes

$$c_i(w.x_i - b) \geq 1 - \varepsilon_i\,, 1 \leq i \leq n \qquad (37)$$

The objective function thus changes as the optimization now involves a tradeoff between a large margin and a small error. For a linear penalty function, the optimization problem becomes

$$min_{w,\varepsilon}\frac{1}{2}\|w\|^2 + C\sum_{i=1}^{n}\varepsilon_i \qquad (38)$$

subject to

$$c_i(w.x_i - b) \geq 1 - \varepsilon_i, \varepsilon_i \geq 0$$

where C is the constant cost coefficient.

The solution w can also be represented as a linear combination of the training points:

$$w = \sum_{i=1}^{n} \alpha_i x_i n_i \qquad (39)$$

Substituting for w in (9) and (10) gives an equivalent optimization problem over α_i instead of w. This is known as the dual form and is given by

$$max_{a_i} \sum_{i=1}^{n} a_i - \frac{1}{2} \sum_{i,j} \alpha_i \alpha_j \, c_i c_j (x_i . x_j) \quad (40)$$

subject to $0 \leq \alpha_i \leq C$ and $\sum_{i=1}^{n} \alpha_i c_i = 0$

4.2.3. Nonlinear SVM

In the case of non-linearly separable data, a nonlinear classifier can be created by applying kernel functions [134]. The original data points are mapped to a higher-order feature space, and (13) can be written as

$$max_{a_i} \sum_{i=1}^{n} a_i - \frac{1}{2} \sum_{i,j} \alpha_i \alpha_j \, c_i c_j k(x_i, x_j) \qquad (41)$$

where $k(x_i, x_j)$ is the kernel function representing the inner dot product of the training points xi and xj. Different kernel functions can be applied by mapping $k(x_i, x_j)$ to different functions. One widely used kernel is the Gaussian or RBF (radial basis function) kernel, with the following mapping:

$$k\left(x_i, x_j\right) = \exp\left(-\gamma \left\| x_i - x_j \right\|^2\right), \gamma > 0 \qquad (42)$$

4.2.4. Parameter selection

The effectiveness of an SVM classifier depends on the selection of the kernel, the kernel's parameters, and the soft margin cost C. For the Gaussian kernel, the two parameters γ and C are often selected by a grid search with exponentially growing sequences of γ and C [134]. The combination of the parameters which gives the best accuracy is selected for training.

4.2.5. Performance evaluation of SVM classifiers

Accuracy, precision, and sensitivity are all statistical measures of the performance of a binary classification test. All possible outcomes of such a test can be represented by a confusion matrix, as shown in Figure 3.3. For example, the following equations provide precision, sensitivity, and accuracy [133]:

$$Precision = \frac{\text{true positive}}{\text{true positive+false positive}} \qquad (43)$$

$$Sensitivity = \frac{\text{true positive}}{\text{true positive+false negative}} \qquad (44)$$

$$Accuracy = \frac{\text{true positive+true negative}}{\text{true positive+false positive}+true\ negative+false\ negative} \qquad (45)$$

		Predicted condition	
	Total population = P + N	Positive (PP)	Negative (PN)
Actual condition	Positive (P)	True positive (TP)	False negative (FN)
	Negative (N)	False positive (FP)	True negative (TN)

Figure 4-4 Confusion matrix

Precision *Eq(43)* is defined by the proportion of true positives to all positive results (true positives and false positives) or the significance of the positive classification. Recall *Eq(44)*, or sensitivity, on the other hand, is defined as the proportion of positive samples that are correctly classified. In other words, it measures the test's ability to detect positives. Sensitivity is defined as the proportion of correctly categorized positive samples. In other words, it indicates the test's capacity to detect positive results [134]. Ultimately, accuracy *Eq(45)* is the proportion of true results, both true positives, and true negatives, in the set.

The **F1 score** attempts to strike a balance between precision and recall. It ranges from 0 to 1 and indicates a classifier's precision and reliability. The higher the F1 score, the better the model's performance. F1 score is the harmonic mean of Precision and Recall and gives a better measure of the incorrectly classified cases than the Accuracy Metric.

$$F1 - score = \left(\frac{Recall^{-1} + Precision^{-1}}{2}\right)^{-1} = 2 * \frac{(Precision * Recall)}{(Precision + Recall)} \tag{46}$$

To summarise the differences between the F1-score and the accuracy,

- Accuracy is used when the True Positives and True negatives are more important, while F1-score is used when the False Negatives and False Positives are crucial.
- Accuracy can be used when the class distribution is similar, while F1-score is a better metric when there are imbalanced classes, as in the above case.
- In most real-life classification problems, imbalanced class distribution exists; thus, F1-score is a better metric to evaluate our model.

Chapter 5. Experimental setup and Data Acquisition

This study aims to evaluate the usability and effectiveness of the chaotic quantifiers of EEG signals on the prognosis of drowsiness. This research has focused on external, non-invasive technologies without ill effects on the tissue being examined. Based on this approach, we have utilized an available off-the-shelf EEG recording device (Brain link EEG system) with a dry sensor measurement system. We have developed algorithms associated with the field of chaotic systems to analyze the measured EEG data for drowsiness prognosis. The system's performance in drowsiness prognosis has been tested and compared by nonlinear methods. Most previous studies utilized the early first collected EEG signals as alert state and compared it with drowsy state data. Still, it is essential to study the EEG signal data during the transition from alert to drowsy state to get precise results. Detecting the transitions from an alert state to a drowsy state is a challenging assignment. The next step is to demonstrate the capability of the device to detect drowsiness in a real-life scenario. We believe that this system will lead to an increase in the performance of drowsiness prognosis.

5.1. Study Subjects

The Simon Fraser University ethical committee approved the recruitment of human subjects for this study (study #30000343). Human subjects were recruited from the students of SFU. Twenty-six volunteers participated in this study. The group consisted of one female and six males (20-50 years old). They had no history of sleep disorder or alcohol abuse. People were asked to normally sleep at least 24 hours before the data recording and take no soporific medications at least three days before the test.

5.2. Proposed System

Figure 5.1 depicts a block diagram of the human-interactive drowsiness prognosis system. The system comprises signal acquisition and data processing, which includes pre-processing, feature extraction, feature selection, and classification.

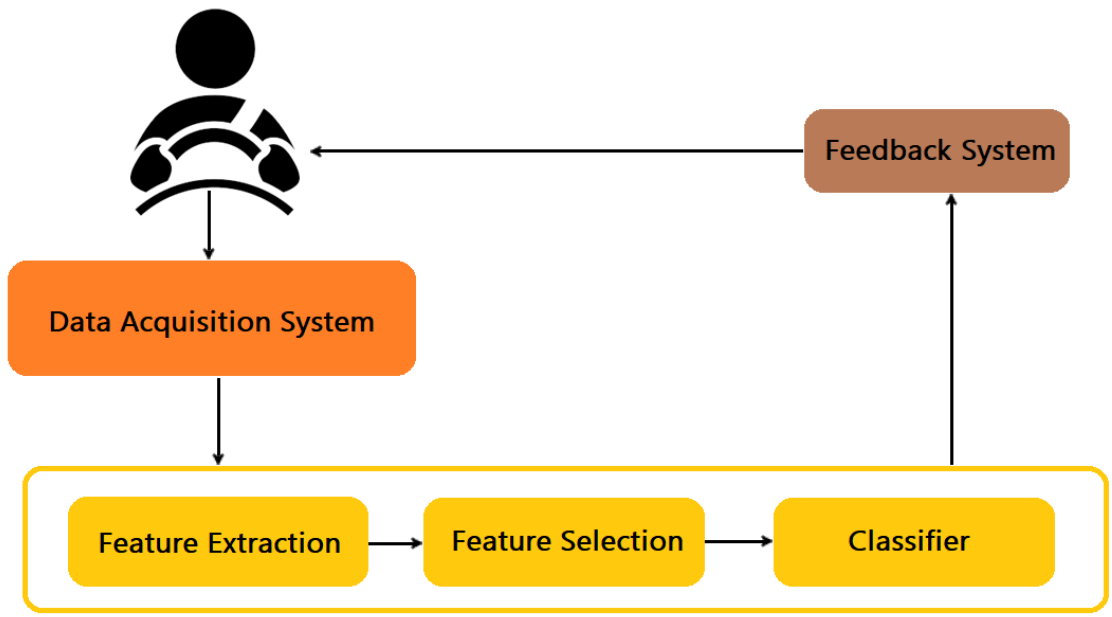

Figure 5-1: Proposed system block diagram

5.3. Data Acquisition System

Future systems should utilize wearable devices with fewer electrodes as much as possible to minimize the cost and processing time. According to studies [136,137], multi-channel systems do not provide a significant advantage over single-channel systems, indicating the viability of a system with improved wearability compared to existing systems involving multiple electrodes. Considering these outcomes, we employed a single-channel data acquisition system for EEG signal collection in this study. This research uses the Brain link EEG system from Macrotellect, Ltd. to record the EEG signal (Figure 5.2).

Figure 5-2 Brainlink EEG System (http://lp2.macrotellect.com/)

Brain link EEG has three dry electrodes with a 500 Hz sampling rate. Various studies [138,139] clearly show that channel FP1 is the most effective channel for identifying driver fatigue and drowsiness. Pertaining these findings, we utilized the FP1 sensor in our research. We needed long-time recordings of EEG data, so we embedded and fixed the sensors in a cap and a blue tooth system transferred the collected data to the computer (Figure 5.3).

Figure 5-3 Acquisition system fix in cap

Placements of recorded channels have been shown in Fig 5.4

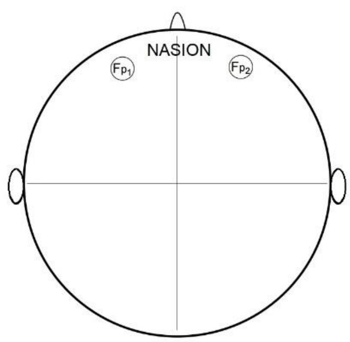

Figure 5-4 EEG Sensors placement

Figure 5.5 shows the utilized EEG data recording system, which contains a wireless EEG cap and a laptop. The EEG cap is powered by a 3.6 V 2600-mAh lithium-ion battery and incorporates a sensory input and processing unit. The captured analog data from the sensory input unit are converted to digital data by the sensory processing unit's built-in 12-bit analog-to-digital converter and stored in the static random-access memory. Then, the digital data are processed for noise and 50 Hz removal by the 32-

bit processor on the sensory processing unit. The pre-processed data are wirelessly transmitted to the laptop via a Bluetooth Low-Energy (BLE) module. The captured data is recorded on a laptop hard disc through an interface software (Nero View) provided by the Brainlink device.

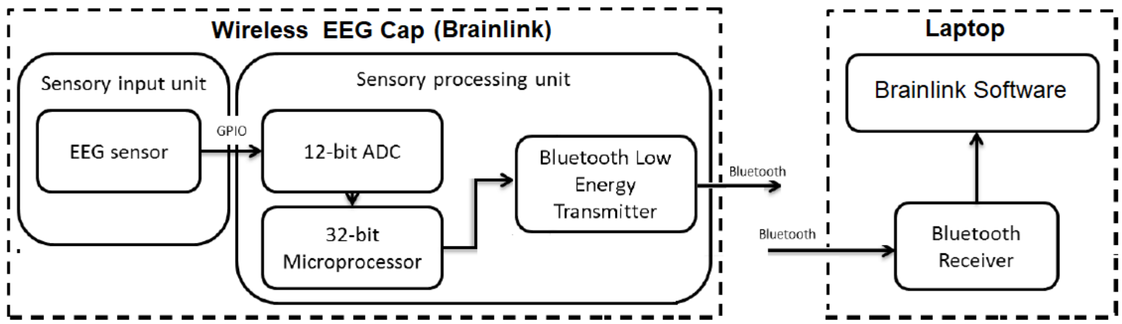

Figure 5-5 EEG data recording system

5.4. Virtual Environment and Data Collection Procedure

Data collection was done in a virtual condition where subjects could feel drowsiness. For this reason, participants were asked to sit relaxed on a chair in front of a computer in a quiet room with normal luminosity while playing a simple driving game to simulate real-world driving conditions until they fell asleep. The laptop's video camera recorded the volunteer's face for the EEG data collection to determine the exact drowsiness (drowsy state) in the data. By comparing the recorded video with the EEG data in each period, awake or drowsiness stats can easily be identified. The EEG data acquisition system was synchronized with a webcam to determine the drowsy state properly. The drowsy state event was marked with visual drowsiness signs, such as slow eye blinks, long eye blink duration, head nodding, or falling asleep. It should be noted that a self-reported drowsy condition was also used to validate the drowsy condition. Some previous studies used subjective sleepiness questionnaires to verify the drowsiness state, which is not an appropriate and reliable technique as the measures in this method change from individual to individual. The biological brain data (EEG) in the form of MATLAB® readable files were collected in the waking state before sleep. Figure 5.6 shows the virtual environment and data collection system.

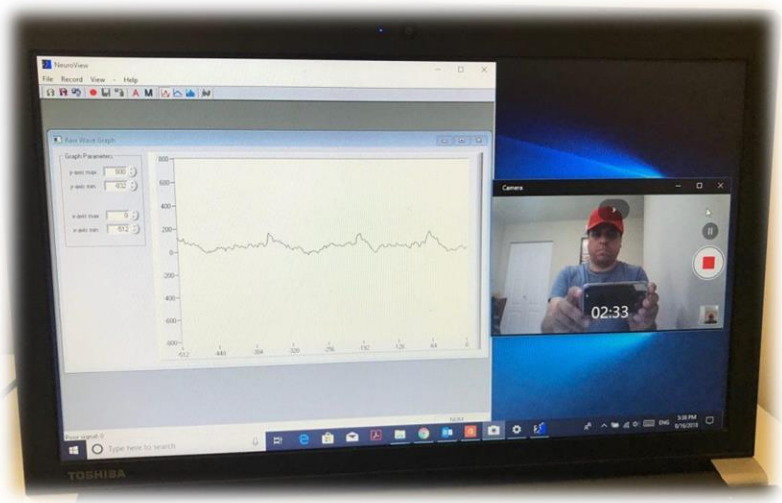

Figure 5-6 Data collection environment

In the following Figure 5.7, two photos of the alert and drowsy states of the participant are extracted from recorded video during the data collection.

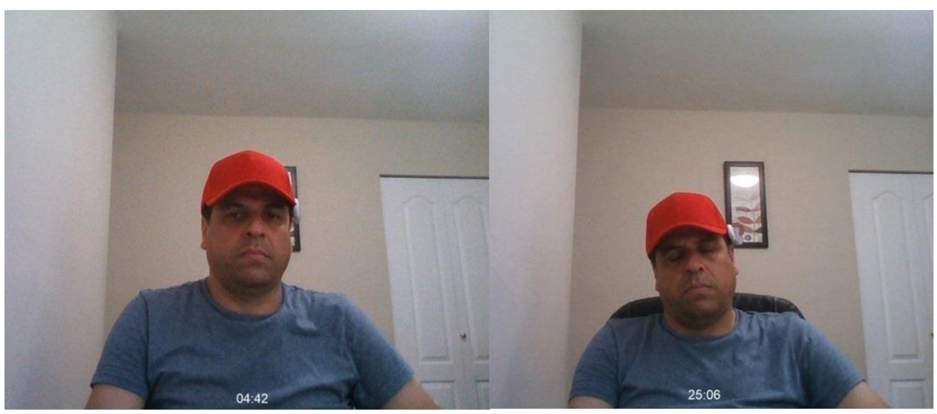

Figure 5-7 Alert and drowsy states

5.5. Data Preprocessing

EEG epoching is a procedure in which specific time-windows are extracted from the continuous EEG signal. These time windows are called “epochs”, and usually are time-locked with respect an event e.g., a visual stimulus. Alert datasets consisted of segments from surface EEG recordings carried out on twenty-five healthy volunteers using a Macrotellt Brain link EEG system. Volunteers were relaxed in an awake state with their eyes open. The drowsy EEG data were recorded from the same volunteers when they started to be drowsy. By comparing the recorded video and self-reported drowsy condition time with the EEG data the drowsiness observation time in data can easily be identified. In order to have sufficient samples in calculating the entropy and fractal dimension as it discussed in chapter 3 the epochs length were selected 180 sec. Two epochs, each containing single-channel EEG segments of 180-sec duration, were composed for the study. The data were analyzed for 180 seconds before the observed drowsy event and 180 seconds after drowsiness. The sampling frequency was 500 Hz with a 12-bit resolution. The first 180 sec of data corresponds to an alert state, and the second 180 sec states the drowsy state. These epochs were selected and cut out from continuous EEG recordings after visual inspection for artifacts, e.g., due to muscle activity or eye movements. EEG signal epoching for awake and drowsy states are given in Figure 5.8.

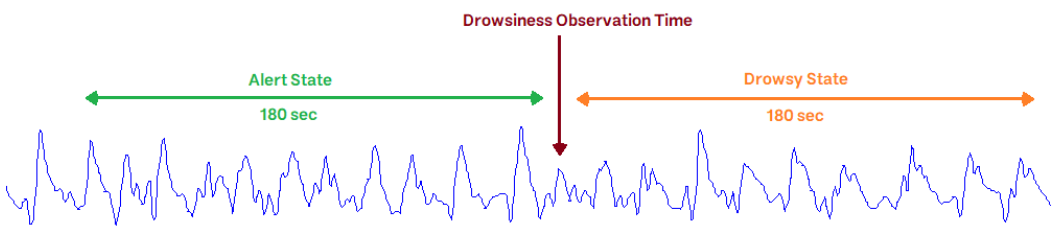

Figure 5-8 EEG signal epoching

In this research, we have analyzed the alert and drowsy states in EEGs using various nonlinear characteristic measures as follows:

- Fractal analysis:
  - Correlation Dimension (CD)
  - Large Lyapunov Exponent (LLE)
  - Higuchi's Fractal Dimension (HFD)
  - Petrosian's Fractal Dimension (PFD)
  - Katz's Fractal Dimension (KFD)
- Entropy analysis:
  - Approximate Entropy (ApEn)

- Sample Entropy (SampEn)
- Fuzzy Entropy (FuzzyEn)
- Permutation Entropy (PermEn)

The characteristics measures are computed using a running window method, as given in Figure 5.9. The sliding observation window is shown in a dark-red frame, which moves through the data as the measures are computed. The data points inside this sliding window are used for feature calculation as the window moves through the data. Therefore, the observation window continuously collapses, and the new observation window's characteristic measure is computed for the data. In our analysis, we have used the window size to be 1500 samples with an overlap of 500 samples between consecutive windows. The window size of 1500 samples corresponds to more than three sec of the signal, and we have used an overlap of 500 samples considering the nonstationarity of the signal. Hence there will be 90 such windows per dataset.

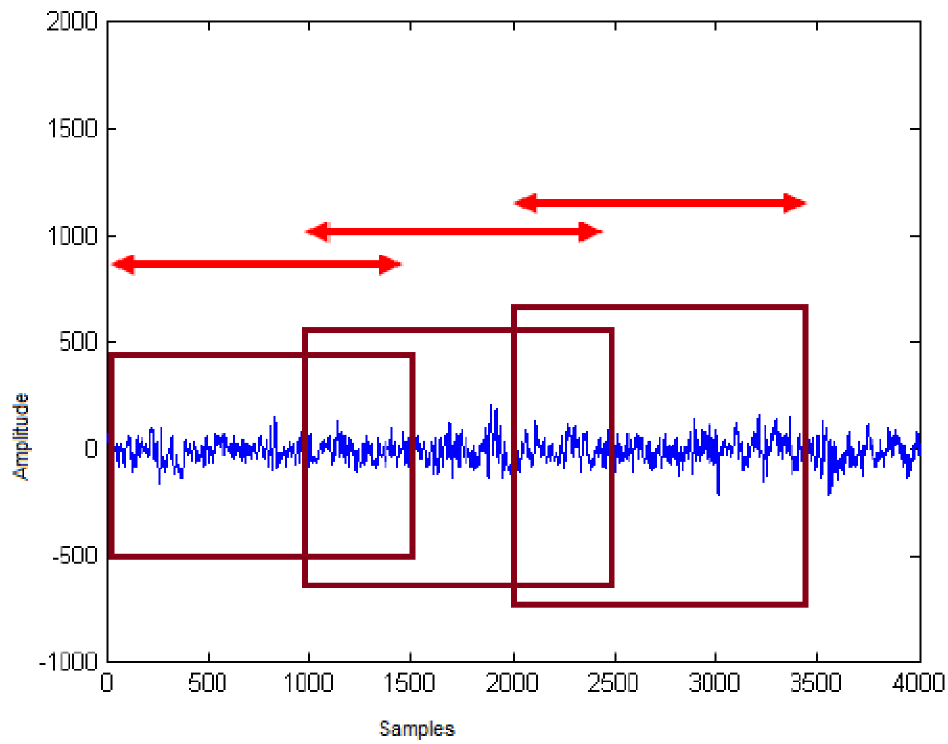

Figure 5-9 Sliding Window

Chapter 6. Results and Discussions

This chapter's primary purpose is to discuss the result of the recommended nonlinear EEG feature extraction methods in chapter three, comparing their performances for drowsiness prognosis, and finally, recommending the most suitable method for drowsiness feature extraction based on the performance.

6.1. Fractal Dimension Analysis

After a review of the methods available in the literature (Chapter three and four) for the analysis of the fractal-like behaviour of the EEG directly in the time domain, we selected five widely used algorithms for the estimation of the fractal dimension of waveforms, Correlation Dimension (CD), Large Lyapunov Exponent (LLE), Higuchi's Fractal Dimension (HFD), Petrosian's Fractal Dimension (PFD), Katz's Fractal Dimension (KFD).

6.1.1. Chaotic Invariants Analysis

The new time series data ($x(t)$, $x(t+\tau)$, $x(t+2\tau)$, . . .,$x(t+(m-1)\tau)$) were created from the time series data by the time shift method.

The optimum embedding parameters are m and τ are calculated using the method described in Chapter two. As mentioned in chapter two, the best approach to calculate the embedding dimension in practical applications is Grassberger and Procaccia algorithm. In this approach correlation dimension (D_2) is calculated for various embedding dimensions, and the minimum embedding dimension (m) is selected when the correlation dimension saturates; then, the minimum embedded dimension plus one is selected as the optimum embedding dimension for system analysis. The graph of D_2 vs. m for awake and drowsy EEG is shown in Figure 3.12.

D_2 saturates at $m_{sat} = 7$; hence the value of the optimum embedding dimension is considered m=8

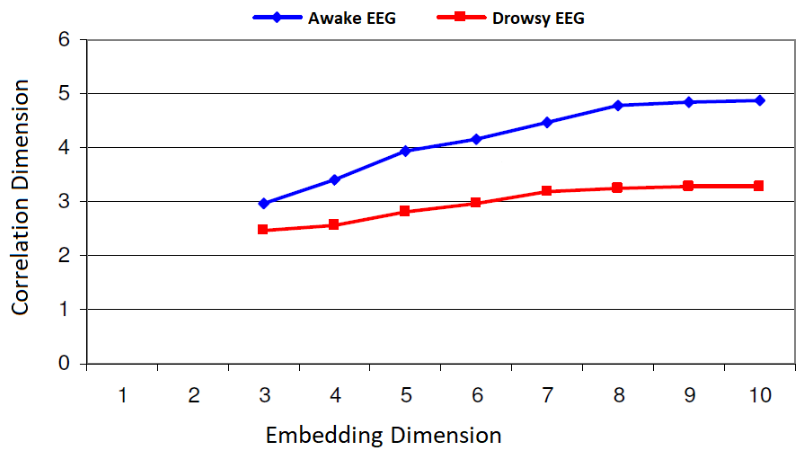

Figure 6-1 Variation of correlation dimension for different embedding dimensions

The mutual information function method was utilized for τ calculation. As mentioned in chapter two, the optimum τ could be extracted from mutual information function plot in different time lags. The mutual information function for awake and drowsy EEG is illustrated in Figure 6.2 and Figure 6.3. The figures show that average mutual information reaches its first minimum in $\tau = 5$.

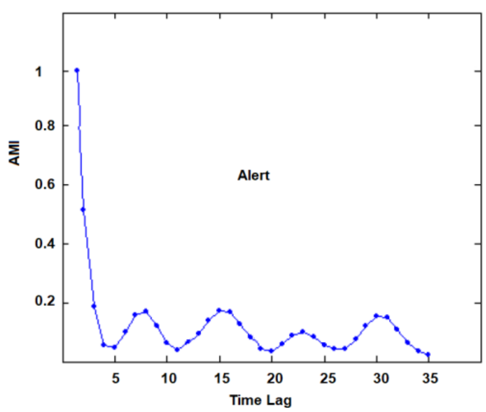

Figure 6-2 AMI of Awake EEG signal

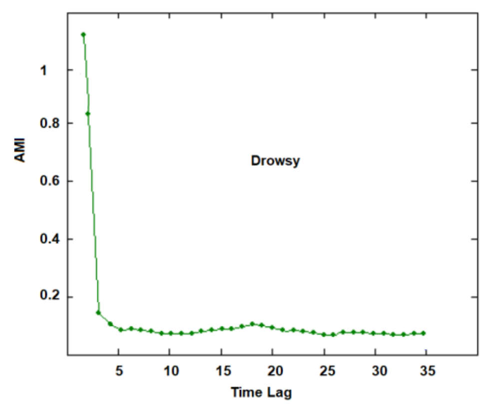

Figure 6-3 AMI of Drowsy EEG signal

Figure 6.4 displays the 3-D plot of the reconstructed attractor of the awake EEG signal with a time delay of $\tau = 5$. Figure 6.5 illustrates the 3-D reconstruction of the drowsy EEG.

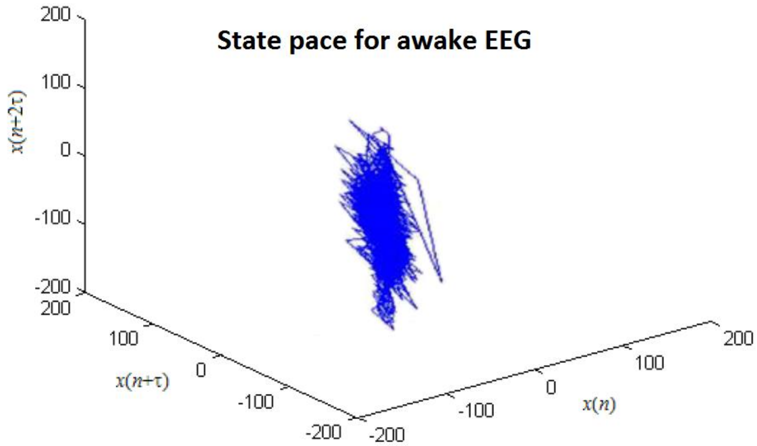

Figure 6-4 Phase-space plot of awake EEG signal

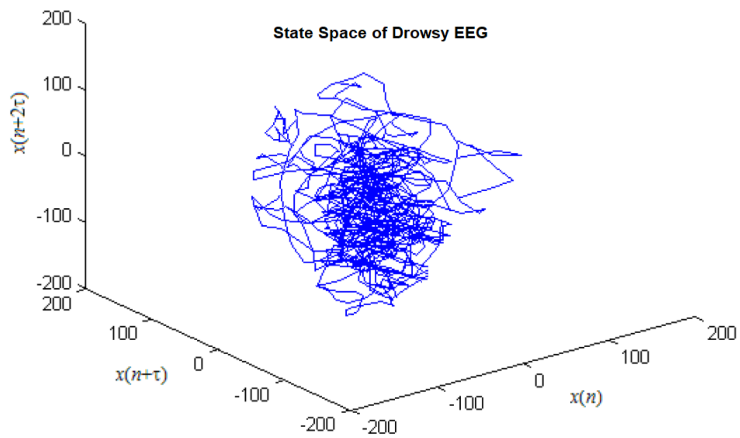

Figure 6-5 Phase-space plot of drowsy EEG signal

6.1.2. Fractal Dimension Result

Each algorithm described in Chapter 3 for fractal dimension calculation was implemented in MATLAB. The FD of the EEG signals is computed using a sliding window approach. An overlapping sliding window with a size of 1500 samples with 500 samples overlap is used. A total of 25 records were analyzed from alert to drowsy state transition subjects. As the sliding window moves, FDs are calculated for each data point that falls within the window, and the mean is used to calculate the signal's FD. Table 6.1 shows the results of the FD analysis of EEGs in alert and drowsy states.

Table 6.1 FD analysis of EEG in alert and drowsy states

Chaotic Measures	Alert state	Drowsy state	p-value
CD	7.2568 ± 0.3667	6.8451 ± 0.182	<0.05
LLE	0.6112 ± 0.0114	0.5945 ± 0.0219	<0.05
HFD	1.7359 ± 0.0223	1.6403 ± 0.0159	<0.05
PFD	1.2952 ± 0.0144	1.2703 ± 0.0153	<0.05
KFD	1.9753 ± 0.0216	1.9026 ± 0.0174	<0.05

Figure 6.6 provides a box plot for each indicator in alert and drowsy states. These results are consistent with Table 6.1 and reveal that all fractal dimension indices generally declined monotonically with transitioning from the alert to a drowsy condition. All indices are effective in terms of qualitative discrimination of awake and drowsy states in EEG signal analysis. However, there are quantitative differences between alert and drowsy indices since each method's concepts are separate. Statistical analysis with a t-test (**$p< 0.05$**) indicates statistical significance supporting our results.

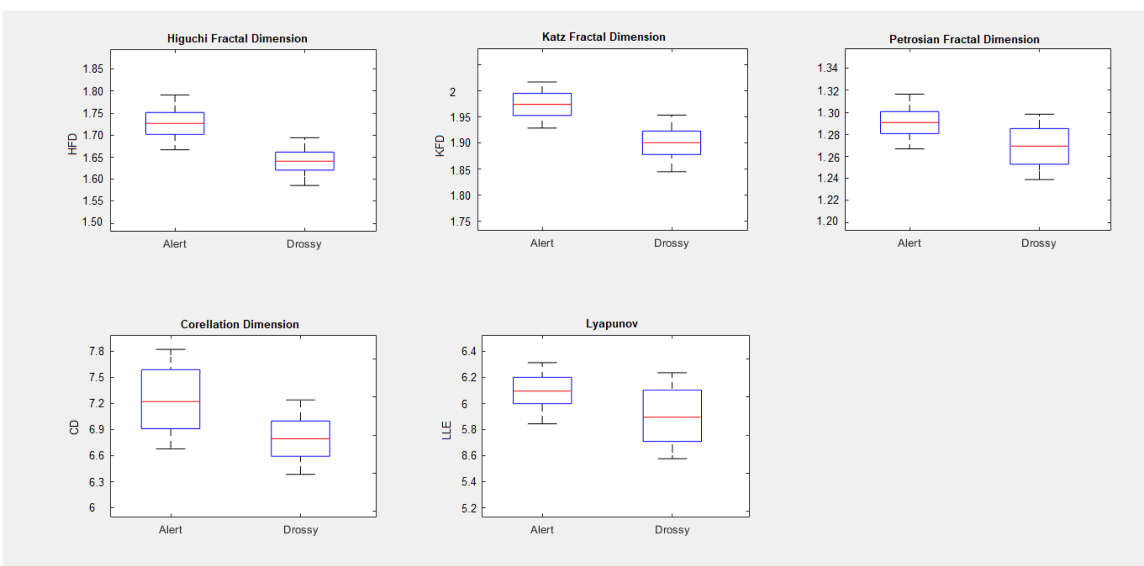

Figure 6-6 Box plot for fractal dimension indicators in alert and drowsy states.

The results of the fractional dimension analysis of the EEG signal from subject number 20 throughout the whole data collection session are depicted in Figures 6.7 to Figure 6.11

respectively for Correlation dimension, Lyapunov exponent, Petrosian fractal dimension, Higuchi fractal dimension and Katz fractal dimension.

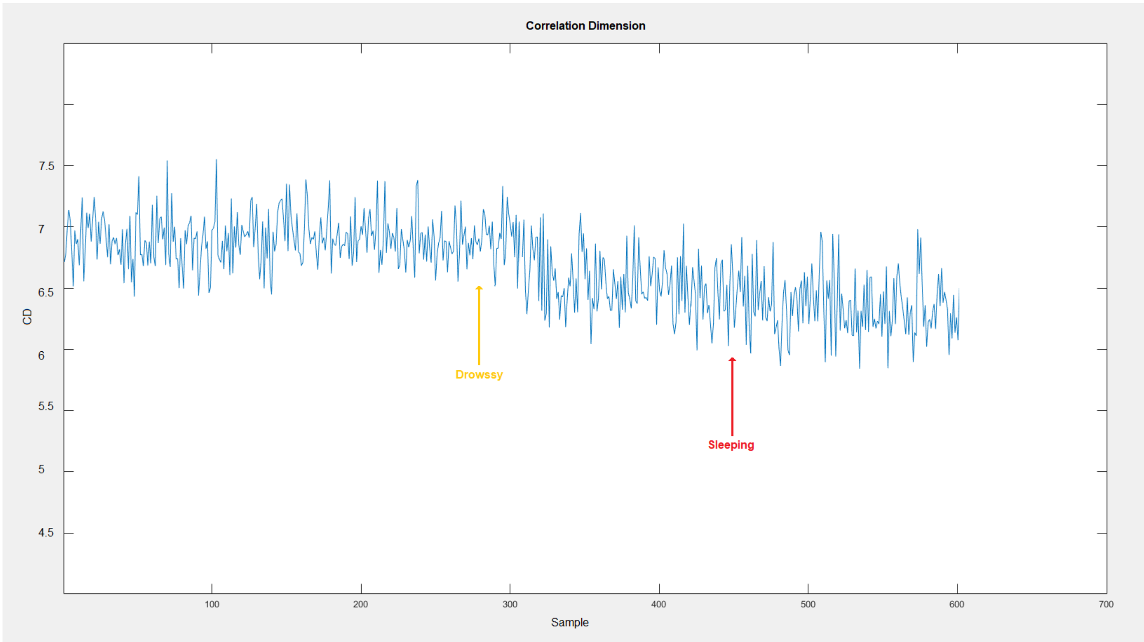

Figure 6-7 Correlation dimension analysis of full sesion EEG signal for subject #20

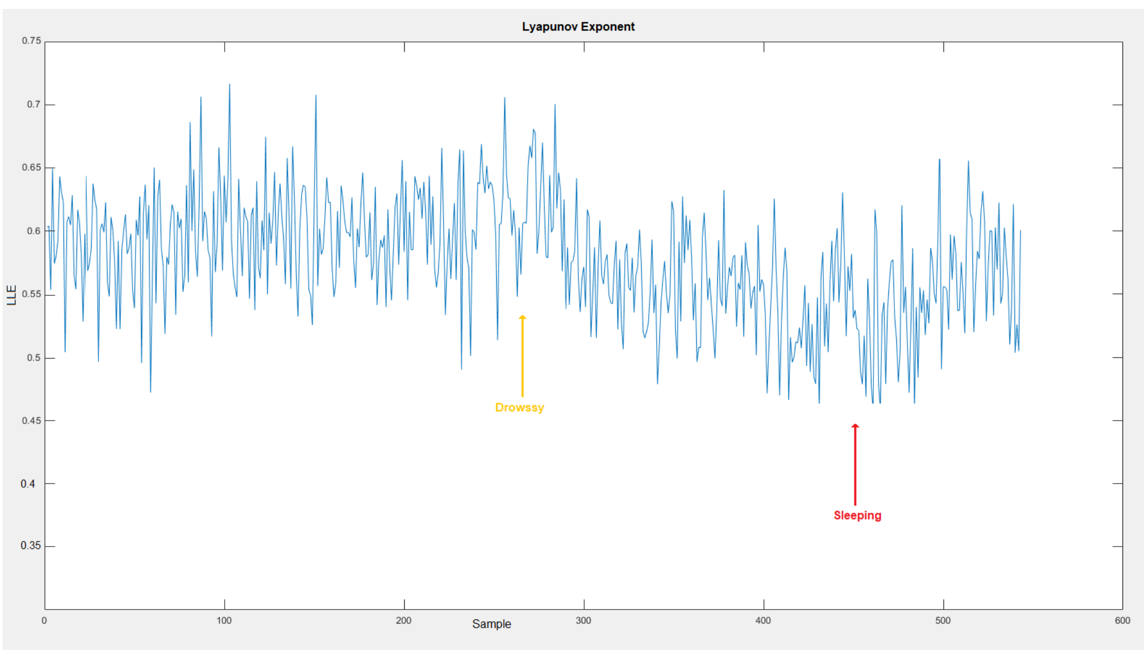

Figure 6-8 Lyapunov exponent analysis of full sesion EEG signal for subject #20

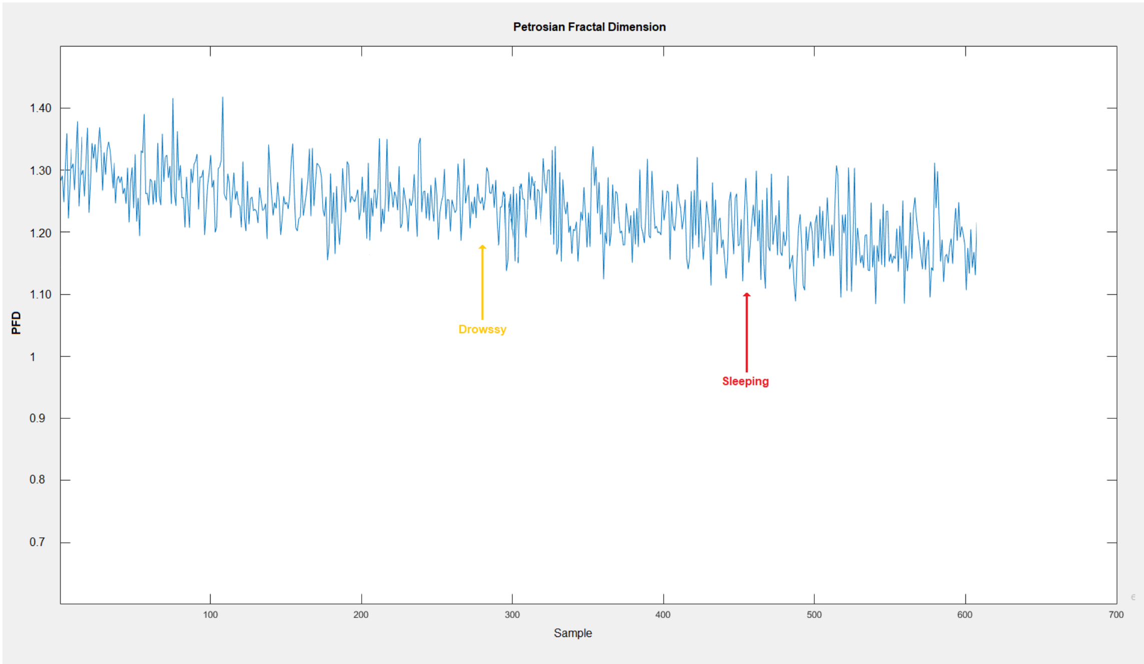

Figure 6-9 Petrosian FD analysis of full sesion EEG signal for subject #20

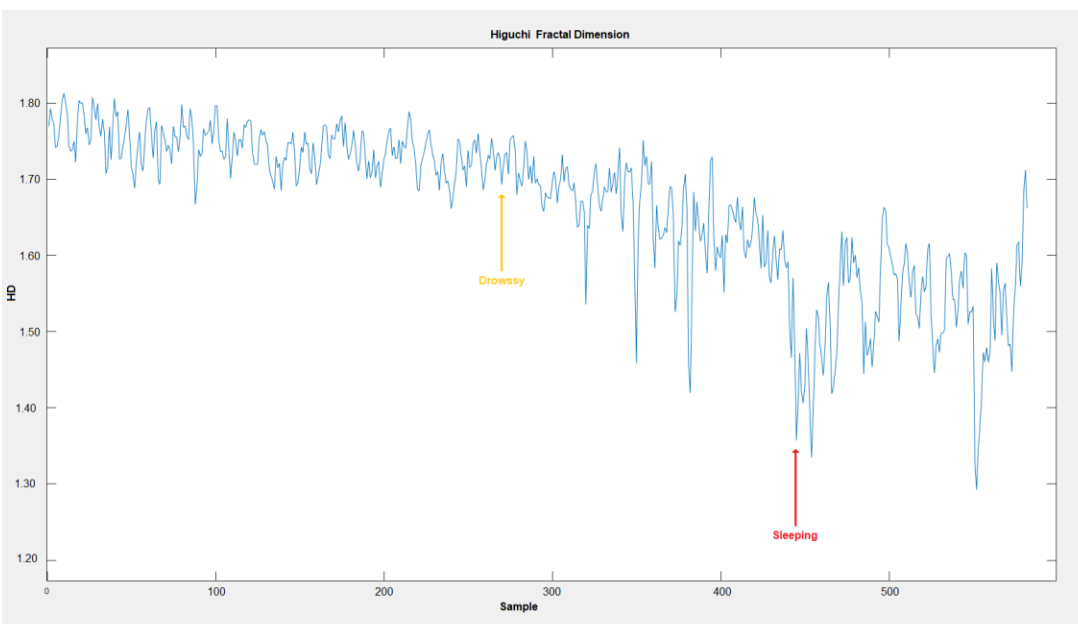

Figure 6-10 Higuchi FD analysis of full sesion EEG signal for subject #20

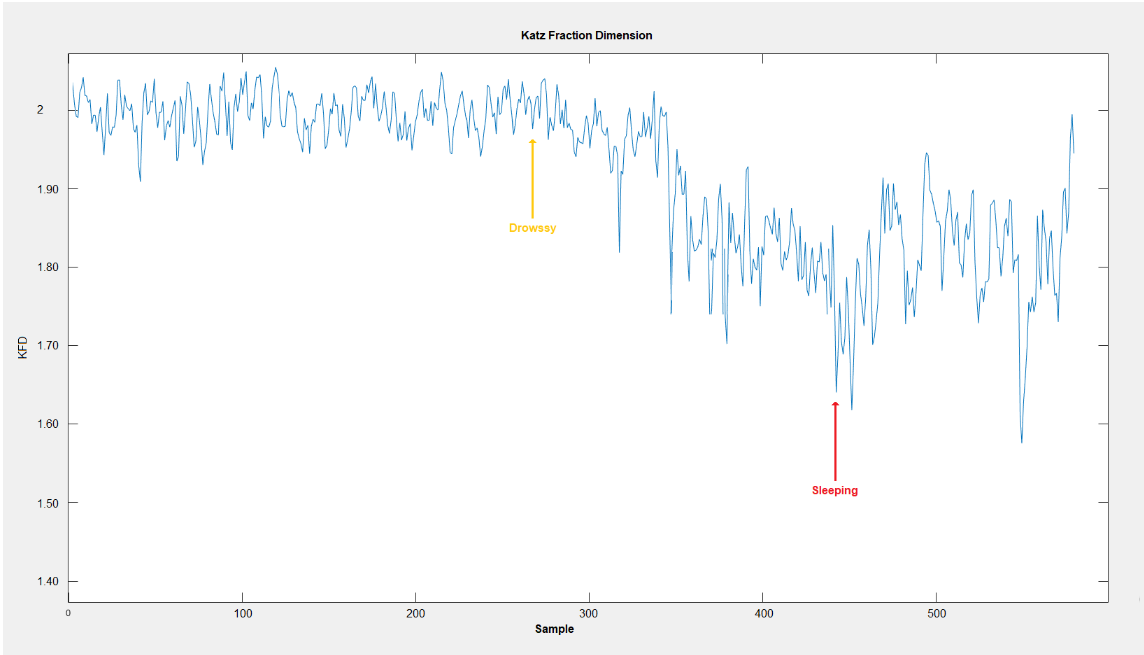

Figure 6-11 Katz FD analysis of full sesion EEG signal for subject #20

6.1.3. Correlation Dimension (CD)

Figure 6.12 and Figure 6.13 demonstrate the variation of correlation dimension (CD) of twenty-five different EEG subjects for alert and drowsy states. The results indicate that the correlation values are higher for alert states with mean and SD values of 7.2568 ± 0.3667, compared with the CD values of the drowsy EEG signals of 6.8451 ± 0.182. This shows that the drowsy EEG signal's complexity is less than the alert state. This shows that the degree of complexity decreases gradually from the alert to a drowsy state. The results agree with the studies [36] on dimension analysis of EEG that dimensionality reduces from awake to sleep. Statistical analysis with a t-test (**$p < 0.05$**) indicates statistical significance supporting our results.

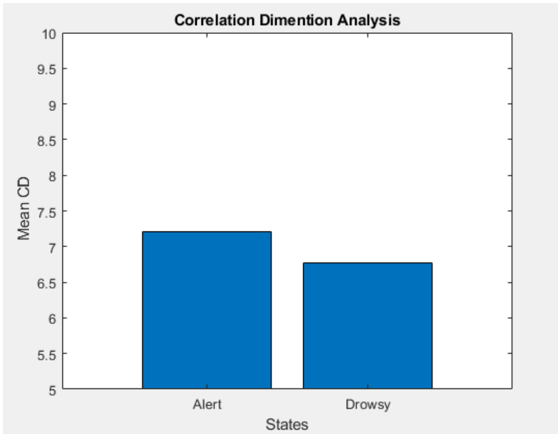

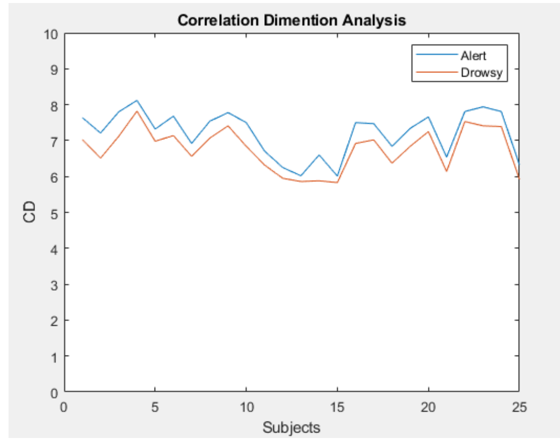

Figure 6-12: Mean value of CD in alert and *d*rowsy states

Figure 6-13 Variation of CD mean value in twenty-five EEG subjects.

6.1.4. Large Lyapunov Exponent (LLE)

Figure 6.13 and Figure 6.14 d shows the variation of the large Lyapunov exponent (LLE) of twenty-five different EEG subjects for alert and drowsy states. The results of LLE are comparable to those observed for CD, as depicted in Figure 6.14. Table 5.1 reveals that the LLE of drowsy EEG (0.5945 ± 0.0219) is less than the LLE of alert EEG (0.6112 ± 0.0114). This indicates that LLE decreases during drowsiness due to the brain's processing flexibility. This suggests that the drowsy EEG has less complexity and fewer independent functional brain processes than the alert state. Positive values for LLE are found in all subjects, indicating chaotic activity.

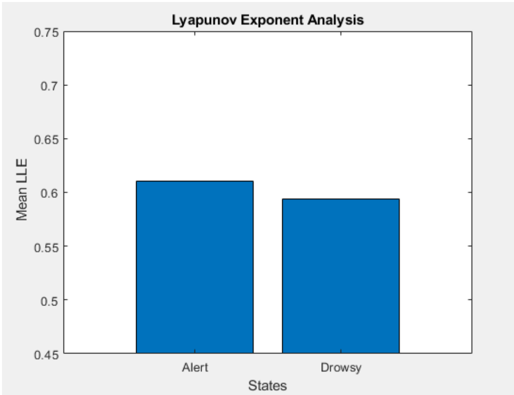

Figure 6-14 Mean value of LLE in alert and drowsy states.

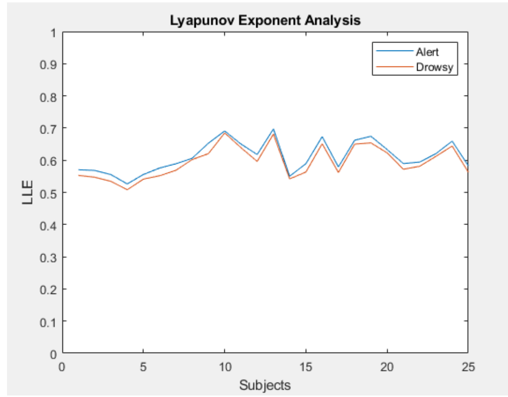

Figure 6-15 Variation of LLE mean value in twenty-five subjects

6.1.5. Higuchi, Petrosian, and Katz's Fractal Dimension

Figure 6.16 and Figure 6.17 shows the variation of Higuchi's Fractal Dimension (HFD) in alert and drowsy EEG. Identical results were obtained for Petrosian's Fractal Dimension (PFD) and Katz's Fractal Dimension (KFD), illustrated in Figures 6.18, 6.19, 6.20, and 6.21, respectively. The results of the Higuchi, Petrosian, and Katz algorithms in table 6.1 indicate a similar trend of decreased FD value for drowsy state EEG compared to alert state EEG. The reduction in FD values characterizes the decrease of brain system complexity for drowsy subjects. FD changes associated with brain states are more critical than FD values.

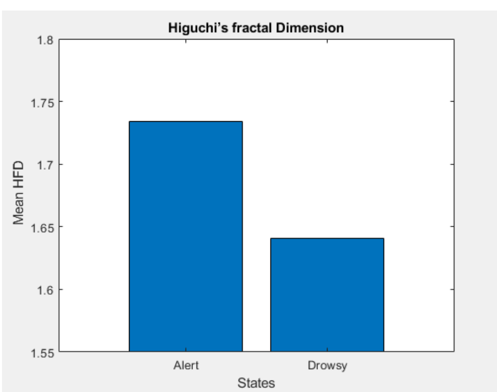

Figure 6-16 Mean value of HFD in alert and drowsy states.

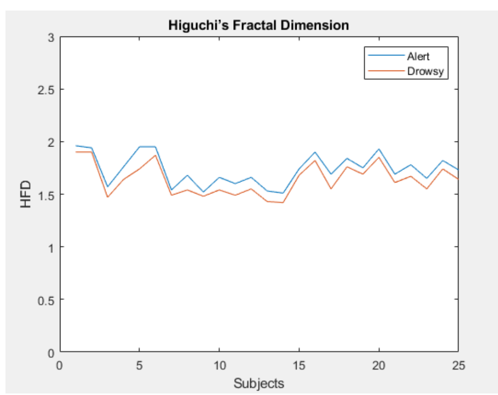

Figure 6-17 Variation of the HFD value in twenty-five subjects.

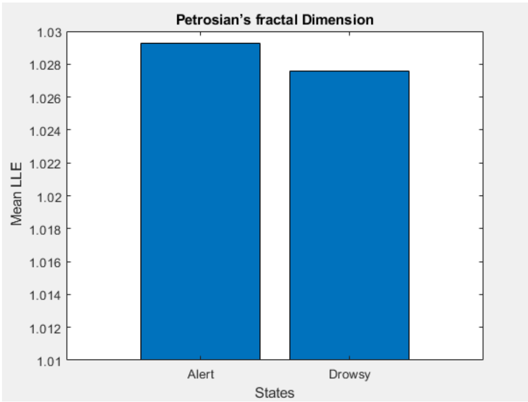

Figure 6-18 Mean value of PFD in alert and drowsy states.

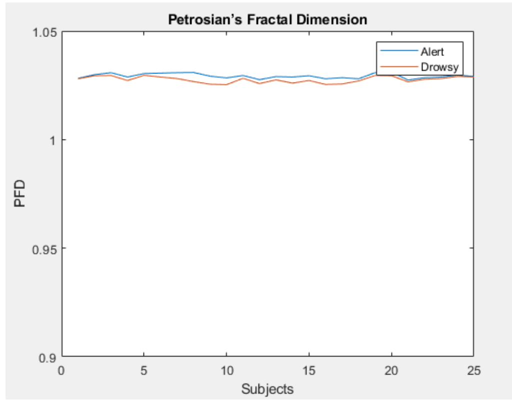

Figure 6-19 Variation of the PFD mean value in twenty-five subjects.

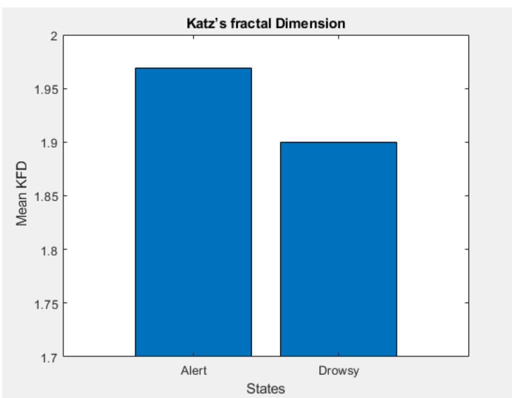

Figure 6-20 Mean value of KFD in alert and drowsy states.

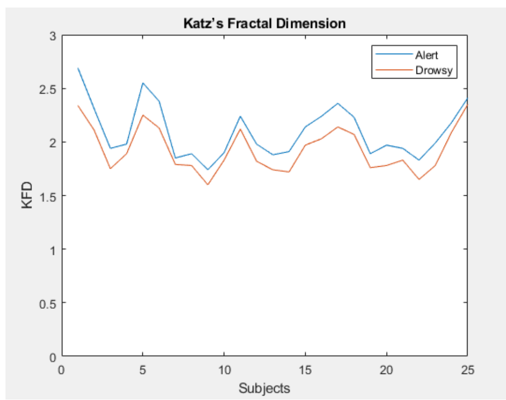

Figure 6-21 Variation of the KFD mean value in twenty-five subjects.

6.2. Entropy Analysis

In addition to the benefits of employing entropy metrics, there are other unresolved issues [128]. A typical objective in investigations of biomedical data is to discriminate between two states of a system. Categorizing pathological and nonpathological data utilizing entropy measurements is one of them. Classification and selecting appropriate data ranges must be better understood [129]. As mentioned in chapter 4, a total of four entropy features, including Approximate entropy (ApEn), Sample entropy (SampEn), Fuzzy entropy (FuzzyEn), and Permutation entropy (PermEn), are selected to analyze their performances in drowsiness prognosis application. These four methods have their advantages. FuzzyEn and PE are less sensitive to signal quality and calculation length [133]. FuzzyEn can resolve greater detail in time series and has a more precise theoretical definition than ApEn and SampEn [134]. Entropy analysis of twenty-five subjects' EEG signals during the transition from alert to the drowsy state has been conducted and tested. We used a sliding window size of 1500 samples with an overlap of 500 samples between consecutive windows. The window size of 1500 samples corresponds to three sec of the signal. A statistical analysis of entropy features was conducted to determine the significance of the distinction between alert and drowsy states. All the selected entropy methods were statistically tested using Analysis of Variance (ANOVA) [132]. Table 6.2 presents the mean and standard deviation (SD) values of these entropies for two different alert and drowsy states of EEG.

Table 6.2 Mean and standard deviation values for entropies in alert and drowsy states

Entropy Measures	**Alert state**	**Drowsy state**	**p-value**
ApEn	1.2531±0.072	1.1237±0.086	<0.001
SampEn	1.652±0.231	1.3324±0.271	<0.001
FuzzyEn	0.5865±0.023	0.5105±0.034	<0.001
PermEn	0.6286±0.014	0.5586±0.024	<0.001

Figure 6.22 provides a box plot for each indicator in alert and drowsy states. These results are consistent with Table 6.2 and reveal that all entropy indices generally declined monotonically with transitioning from the alert to a drowsy condition. All indices are effective in terms of qualitative discrimination of awake and drowsy states in EEG signal analysis. However, there are quantitative differences between alert and drowsy indices since each method's concepts are separate. Statistical analysis with a t-test (**$p < 0.001$**)

indicates statistical significance supporting our results.

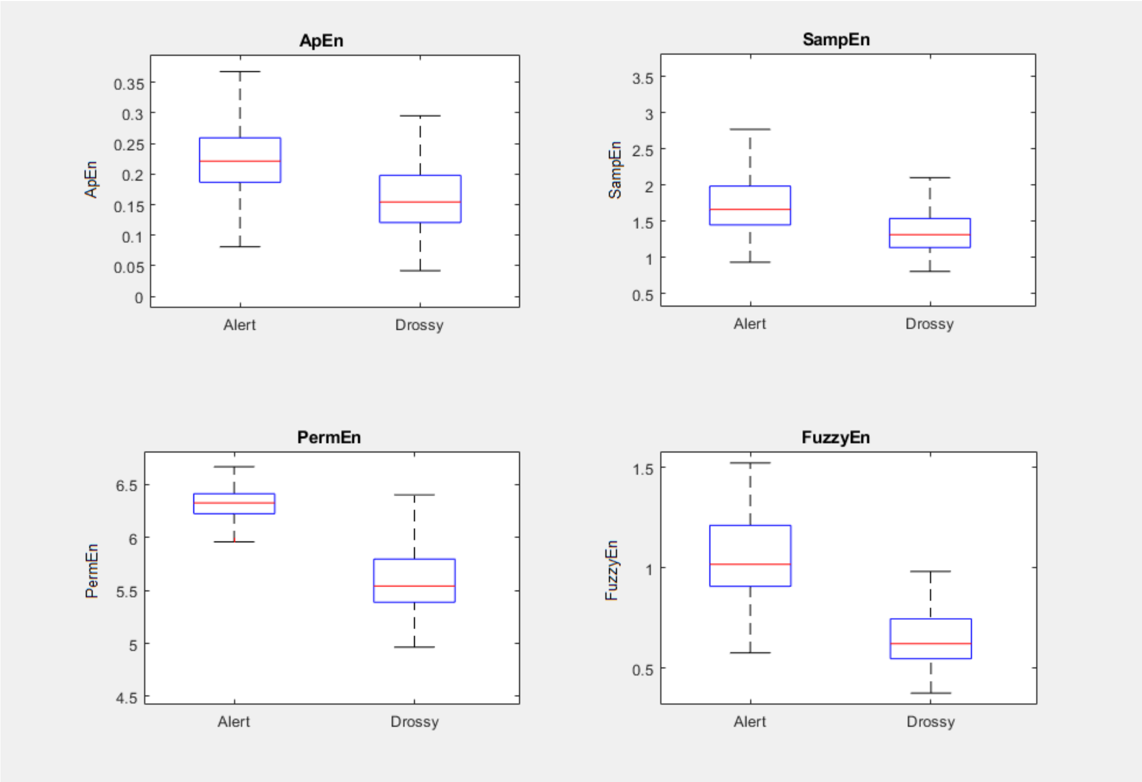

Figure 6-22 Box plot for entropy indicators in alert and drowsy states.

6.3. Discussion and Feature Selection

Feature extraction and selection are different; feature extraction creates new features from functions of the original features, while feature selection returns a subset. The process of selecting a subset of relevant and effective features (predictors) for use in model construction or classifier is referred to as feature selection. Feature selection techniques simplify models, reduce training time, and avoid dimensionality.

Even though each fractal dimension and entropy method has theoretical advantages regarding the characterization of EEG data, we must evaluate the functional performance from various aspects to select the more reliable and accurate feature as classifier input. We assessed these methods concerning accuracy, efficiency (computational time), and prediction time.

6.3.1. Fractal measures assessments

6.3.1.1 Comparison of accuracy:

The Katz algorithm has a higher FD value for drowsy and alert EEG than other methods. Katz and Higuchi's algorithms perform better in discriminating drowsy EEG from alert EEG. As shown in Figures 6.6 and 6.23, the margin between the mean FD values of alert and drowsy when using the Petrosian and LLE algorithms is minimal, making it difficult to distinguish between alert and drowsy states. Even though the mean FD value of the correlation dimension for the alert is high, the results are inconsistent.

The transition between alertness and drowsiness is crucial for drowsiness prognosis. We investigated the ability of FD methods to trace this point. The absolute slope values (mean ± SD) of the linear-fitted polynomials vs. time were calculated for these indices. Figure 31 shows the changes in each index during the transition. As can be seen, the absolute slope value for Katz (0.433) is the largest, followed by HFD (0.392).

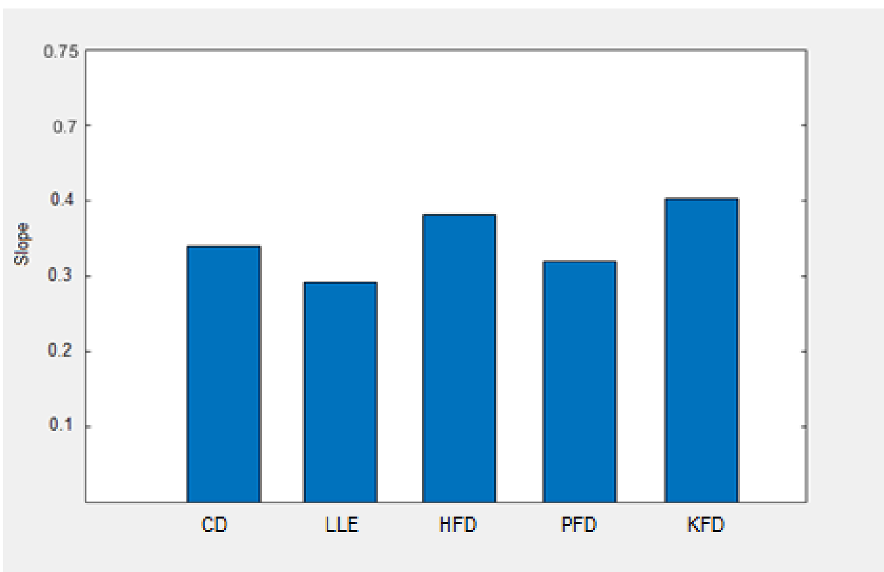

Figure 6-23 Absolute slope of the linear-fitted polynomials vs. time for FD indices

6.3.1.2. Comparison of drowsiness prediction time:

Fig 6.24 shows Higuchi's fractal dimension during the transition from an alert state to a drowsy state. To estimate the drowsiness prediction time before sleeping, we need to determine the sleep and drowsy time. The sleep time of the subject is determined by synchronizing the recorded movie and EEG signal. Drowsy time is defined as the time when the FD amount falls below the mean. This method was employed to calculate the drowsiness prediction time using various FD methods, and the results are shown in Figure 6.25. The results show that Higuchi and Katz's algorithms outperform the other methods in terms of drowsiness prediction time.

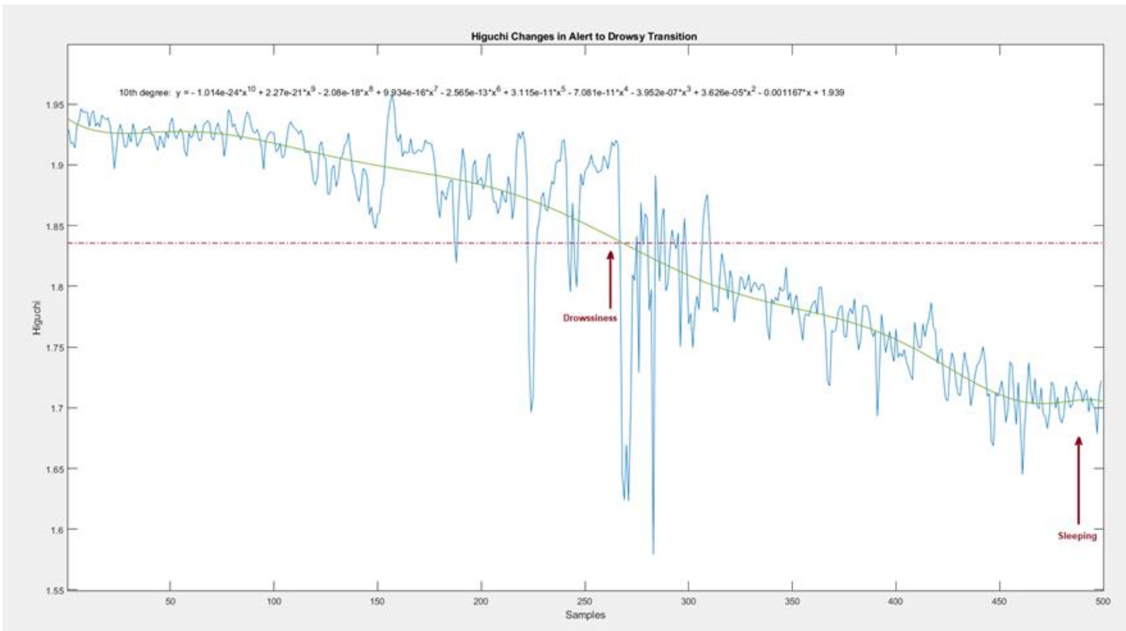

Figure 6-24 Higuchi fraction dimension Changes in transition from alert to a drowsy state

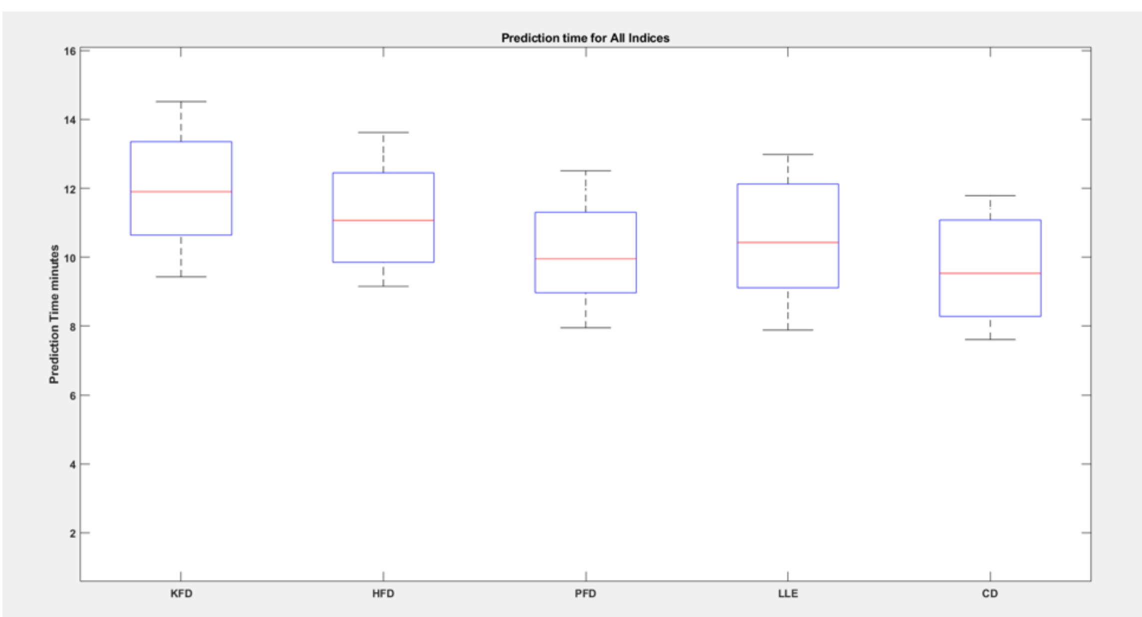

Figure 6-25 Drowsiness Prediction time before sleeping for FD indices

6.3.1.3 Comparison of computational time:

Table 6.3 compares the run time of the methods. Results indicate Katz's method is computationally faster, while Higuchi's and Petrosian's are on the second and third orders of magnitude, respectively. The runtime of the CD and LLE methods is the slowest among the FD methods. As discussed in chapter three, spatial dimensionality, including correlation dimension and Lyapunov exponents, requires reconstruction of the time series state space to calculate fractal dimension, which increases the computational burden and slows the algorithm. The test computer's configuration was an Intel Core i7 CPU, at 3.40 GHz, with 8 GB of RAM, running Windows 10 Professional operating system.

Table 6.3 Computational time for FD Indices

Fraction Dimension index	Run time (sec)
CD	3.68±0.356
LLE	2.832±0.438
HFD	0.318±0.024
PFD	0.469±0.037
KFD	0.243±0.018

6.3.1.4. Conclusion

Exploring brain complexity directly in the time domain without phase space reconstruction would benefit EEG nonlinear analysis. According to the result and performance comparison of the different FD methods in the past section, direct estimation of the fractal dimension with Higuchi and Katz algorithms are preferable. In contrast, using the correlation dimension and Lyapunov exponent is discouraged due to the slow run time and experiment inaccuracies. Higuchi and Katz’s algorithms provide the most accurate values of the FD. They are computationally fast to discriminate alert and drowsy states of EEG signals in comparison with other FD methods. Based on these results, Katz and Higuchi’s methods have been chosen as the best chaotic fractal dimension indicator for feature extraction in drowsiness prognosis.

6.3.2. Entropy measures assessments

6.3.2.1. Comparison of Accuracy*:*

To examine the effectiveness of the indices to discriminate alert and drowsy phases, Figure 6.22 results are helpful. The overlap of PermEn and FuzzyEn values between the alert and drowsy states were smaller than the other indices. This means the PermEn and FuzzyEn have a better ability to separate these states and a greater robustness for prognosis.

We investigated the ability of entropies to trace this point. The absolute slope values (mean ± SD) of the linear-fitted polynomials vs. time were calculated for these indices. Figure 6.26 shows the changes in each index during the transition. As can be seen, the absolute slope value for PermEn (0.381) is the largest, followed by Fuzzy (0.326).

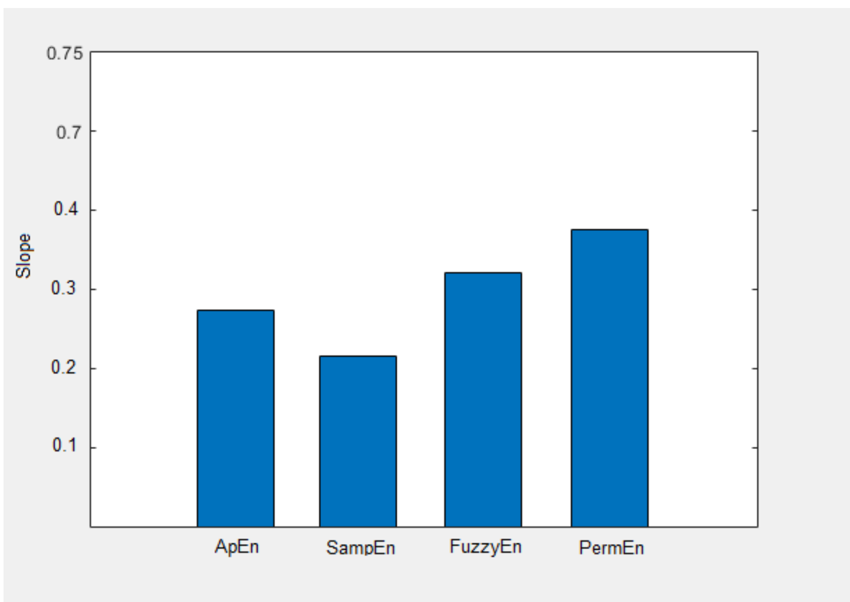

Figure 6-26 Absolute slope of the linear-fitted polynomials vs. time for entropy indices

6.3.2.2. Comparison of drowsiness prediction time:

To estimate the drowsiness prediction time before sleeping, the sleep and drowsy time have been determined. The sleep time of the subject is specified by synchronizing the recorded movie with an EEG signal. Drowsy time is defined as the time when the entropy value falls below the mean. This method was employed to calculate the drowsiness prediction time using various entropy methods, and the results are shown in Figure 6.27**.** The prediction time values of FuzzyEn (12.56 minutes) and PermEn (11.83 minutes) were higher than other indices.

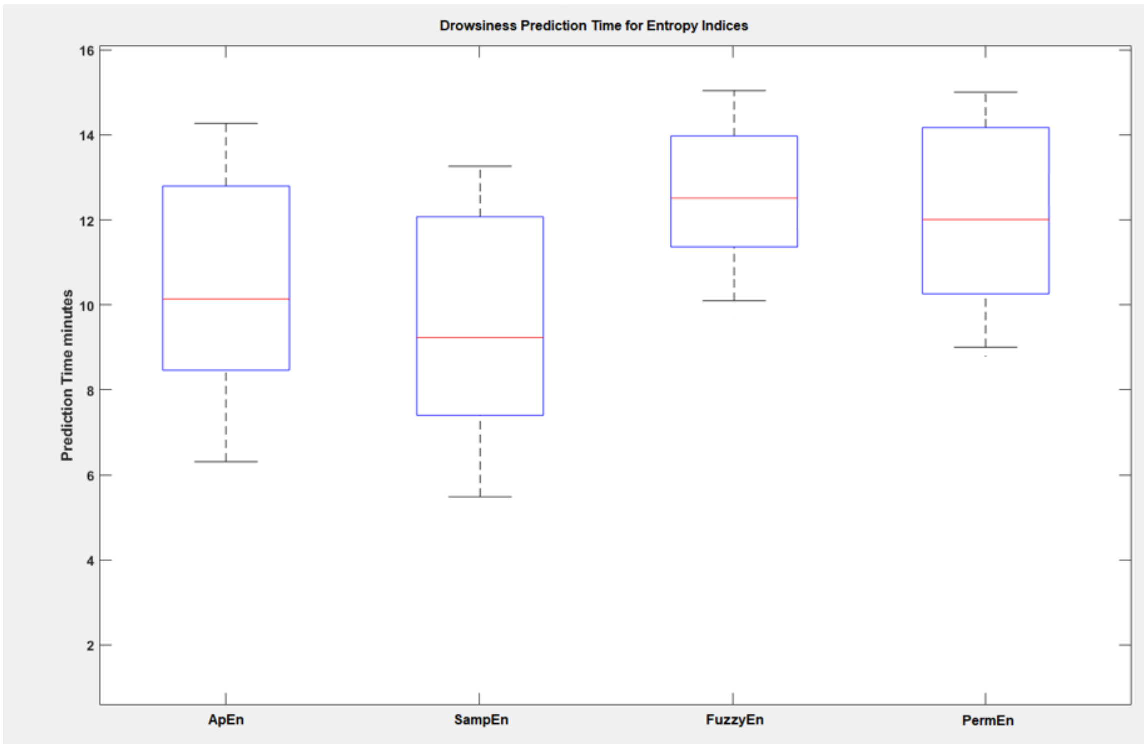

Figure 6-27 Drowsiness Prediction time before sleep for Entropy indices

6.3.2.3. Comparison of computational time:

To compare the computational time performance of each index, the run time of each index for the same subject was calculated. The computing time for 6 min of EEG data compared for each index is given in Table 6.4.

The fastest index was PermEn (0.385 ± 0.012 s). The ApEn and FuzzyEn run times were (1.751 ± 0.013 s) and (1.628 ± 0.037 s) respectively. The SampEn (1.751 ± 0.16 s) was the slowest. The test computer's configuration was an Intel Core i7 CPU, at 3.40 GHz, with 8 GB of RAM, running Windows 10 Professional operating system.

Table 6.4: The computing time for different entropy indices for 6 min data length.

Entropy index	Run time (sec)
ApEn	1.28±0.082
SampEn	1.751±0.016
FuzzyEn	1.628±0.037
PermEn	0.385±0.012

6.3.2.4. Conclusion

In this section, we investigated the performance of four entropy algorithms to assess the EEG signal for drowsiness prognosis, including ApEn, SampEn, FuzzyEn, and PermEn. Twenty-five data sets were employed as the test samples to assess the effectiveness of mentioned entropy indicators. To evaluation of each entropy index, four measures were considered.

The boxplots of indices were used to evaluate their ability to discriminate between alert and drowsy states. The results indicated that PermEn performed better than the other indices at this level. Furthermore, the performance for estimating the point of transition was considered. Although all the entropy measures could distinguish between alert and drowsy states, the speed of transition (slope) between the two states was fastest for PermEn and Fuzzy, while SampEn had the slowest transition. The subsequent evaluation was the drowsiness prediction time before sleep. The results demonstrated that the FuzzyEn and PermEn indices are superior in predicting drowsiness. The last assessment used was the computing time and speed of the algorithm. The results indicated that the PermEn index is the entropy index with the fastest algorithm, and SampEn was the slowest.

The excellent performance of FuzzyEn and PermEn indicates their potential usefulness in drowsiness prognosis.

6.4. SVM Classifier for drowsiness prognosis

The characteristic measures of the EEG signals discussed in Chapter 4 are evaluated for suitability to do classification. The classification is done using the classification technique discussed in chapter 3. The four selected features in section 6.3, including HFD, KFD, FuzzyEn, and PermEn, are used as inputs to the classifier for drowsiness detection. After feature extraction, the classification is done using the SVM classifier to classify "alert" and "drowsy" EEG epochs automatically. The performance of this classifier is discussed and compared in this chapter.

The trained SVM was tested using the testing set of EEG data to evaluate its accuracy in distinguishing between 'alert' and 'drowsy' EEG. The trained SVM program was also evaluated for its accuracy and reliability in identifying the turning point between alertness and drowsiness in experimental data. Data sequences corresponding to alertness to drowsiness transitions were extracted from the experimental dataset. Each sequence was divided into 10-s epoch sub-segments. The SVM program classified each sub-segment as alert or drowsy. These sub-segments were re-combined to find the turning point identified by the SVM program along the data segment. This testing method would measure the turning point in 10-second epoch divisions. This turning point identified by the SVM program would be compared to manual classification with one of three possible outcomes. In comparison to manual classification, the SVM program could identify the turning point at the same epoch as manual scoring (a "correct" predictor), earlier epochs (an "early" predictor) or later epochs (a "delayed" predictor).

The four features are integrated and constructed in the input vector $I = (I_1; I_2; I_3; I_4)$. Since these four vectors are 2-dimensional, we can establish an 8-dimensional input feature vector I. As the different features have different meanings, it is necessary to normalize the input feature vector by:

$$F_i = \frac{I_i - \mu_i}{\sigma_i}$$

Where μ_i and σ_i are the average and standard deviation of the *i* th feature.

The dataset was randomly divided into five subsets with similar samples from each class to assess the classifier performance. Four subsets are utilized as training data, and one subset as testing data. This procedure is performed five times. A five-fold cross-validation technique is applied to get the optimal parameters C and g for SVM in each process. The classification accuracies for separate processes and the average and standard deviation of five times are demonstrated in Table 6.5.

Table 6.5 classification accuracies and F1 score for separate and feature fusion processes

		HFD (F_1)	KFD (F_2)	FuzzyEn (F_3)	PermEn (F_4)	F
1	ACC	86.45	91.05	88.93	85.64	97.39
	F1Score	0.884	0.920	0.896	0.832	0.931
2	Acc	75.21	85.38	76.38	78.42	95.36
	F1Score	0.914	0.947	0.852	0.908	0.928
3	Acc	69.56	72.64	81.46	80.67	96.72
	F1Score	0.833	0.946	0.871	0.866	0.904
4	Acc	84.38	81.54	80.29	82.74	95.59
	F1Score	0.886	0.915	0.931	0.896	0.929
5	Acc	78.49	76.44	77.56	76.05	96.43
	F1Score	0.842	0.940	0.893	0.919	0.938
Mean	Acc	78.82±6.8	81.41±7.25	80.92±4.91	80.70±3.72	96.30±0.83

Table 6.5 indicates that feature fusion results in an average accuracy of %96.30, which is 14.89 % higher than the second-best accuracy. The average accuracies of the rest three input features (F_1, F_4, F_3) are 78.82, 80.92, and 80.70, respectively. Average accuracy results indicate that fusion feature classification outperforms single features. The reduced deviation in feature fusion demonstrates that the performance of this method is more stable than that of a single feature.

Several research groups have investigated driver drowsiness detection using EEG signals. The classification performance employed in their studies, listed in Table 6.6, indicates that our results based on features fusion of one electrode were superior to the results of many other classification methods.

Table 6.6 Performance comparison of the previous works.

Author	Domain	Method	Classifier	Accuracy	F1 Score
Anitha [140]	Frequency	FFT	SVM	87.2	0.864
Belakhdar[137]	Frequency	FFT	ANN	88.7	0.83
Correa [148]	Frequency Time-Frequency	FFT, DWT	ANN	86.7	0.889
Correa [141]	Frequency Time-Frequency	FFT, DWT	ANN	87.6	0.852
Xiong [149]	Time	AE & SE	SVM	90	0.81
Chai R [150]	Time	Entropy	ANN	88.2	0.93
Proposed	Time	FD-EN	SVM	96.30	0.93

The average highest recognition rate in this work was 96.30%, which could meet the needs of daily applications.

Chapter 7. Conclusion and Feature works

7.1. Conclusion

Truck driver drowsiness is one of the leading causes of catastrophic accidents in the mining industry, resulting in irreversible economic, health, and life losses. Hence, it is crucial to use an automated system to monitor and predict drivers' drowsiness in the mining industry. Current drowsiness monitoring and detecting methods have been focused on vehicle and behaviour-based measurements. Several studies have been carried out on drowsiness detection with linear EEG analysis. Still, since the linear models cannot capture the underlying nonlinearity in the original signal, outcomes were unreliable. Few nonlinear analyses have been conducted to detect drowsiness, and all algorithms have been applied separately on awake and drowsy states; no study has been conducted on the transition from alert to drowsy state.

In this research, EEG signals are characterized using different nonlinear measures. The EEG signals during the transition from alert to drowsy of subjects analyzed using the nonlinear time series analysis techniques expecting to extract quantitative measures that can reliably distinguish the EEG of an epileptic subject from that of a normal subject. The results of our analysis demonstrated the potential of complexity measures such as C*D*, LLE, HFD, KFD, PFD, ApEn, SampEn, FuzzyEn, and PermEn in quantifying the EEG signals of alert and drowsy subjects. The experimental results reveal that drowsiness significantly affects fractal and chaotic entropy quantifiers. It is clearly shown that the values are higher for alert subjects than for drowsy subjects. The statistical results also support the discriminating ability of these measures in identifying alert and drowsy EEG signals. These measures could be used as a drowsiness indicator and serve as quantitative descriptors of EEG in automatically identifying drowsy EEG signals. The analysis of nonlinear dynamics in EEG signals serves as an aid in understanding the underlying physiological processes in the brain. The experimental outcomes pinpoint four indices from fractal and entropy measures as the most sensitive and robust features for drowsiness prognosis: Higuchi's Fractal Dimension, Katz's Fractal Dimension (KFD), Fuzzy Entropy (FuzzyEn) and Permutation Entropy (PermEn). A fusion of features is considered for classifying EEG signals to integrate the strengths of the four proposed indices. The SVM architecture classifier is used for the classification of EEG signals. In several experiments, the overall accuracy of the developed drowsiness prognosis system is about 96.30%.

7.2. Future Work

The research accomplished in this thesis should be continued in the following directions:

- The neurobehavioral performance and awake EEG are phase-locked to the circadian rhythm and adjusted by the elapsed time awake. Future work should apply the measures to data sets from different circadian phases and validate this study's results.

- The EEG datasets considered in this study are derived from the FP2 electrode of EEG records. Since not all electrodes carry the information of interest, comprehensive research should be done to identify the EEG sensor’s best location for the proposed technique.

- This study is limited to a small group of subjects, and a more extensive study is needed to give more robust statistics. To ensure the statistical relevance of the results, the dataset must be expanded in future work. The results can be further enhanced by adjusting the hyperparameters and using larger sample sizes.

- Due to the urgency of warning the driver of a potential hazard, future work on the proposed solution should include real-time feedback. This would require real-time data acquisition and visualization techniques, as well as rapid classification and feedback. The final solution must also incorporate auditory, visual, or vibratory feedback to alert the driver of drowsiness.

Reference list

1. Mosby's Medical Dictionary (10th ed.), (2016). Retrieved from https://medical-dictionary.thefreedictionary.com/drowsy

2. Weiner, I. B., & Craighead, E. W. (2010). The Corsini Encyclopedia of Psychology, Volume 1 (4th ed.). New York, USA: Wiley.

3. American Academy of Sleep Medicine. (2005). International Classification of Sleep Disorders: Diagnostic & Coding Manual (2nd ed.) page 343. Retrieved from https://web.archive.org/web/20110726034931/http://www.esst.org/adds/ICSD.pdf

4. Poudel, G. R., Innes, C. R., Bones, P. J., Watts, R., & Jones, R. D. (2014). Losing the struggle to stay awake: divergent thalamic and cortical activity during microsleeps. Human brain mapping, 35(1), 257–269. https://doi.org/10.1002/hbm.22178

5. USA National Highway Traffic Safety Administration. (2016, March). NHTSA Drowsy Driving Research and Program Plan. Retrieved from https://www.nhtsa.gov/sites/nhtsa.dot.gov/files/drowsydriving_strategicplan_030316.pdf

6. Purves, D., Augustine, G. J., Fitzpatrick, D., Hall, W. C., LaMantia, A., Mooney, R. D., White, L. E. (2017). Neuroscience (6th ed.). Sunderland, USA: Sinauer Associates, Inc. Publishers,

7. Steriade, M., & Llinás, R. R. (1988). The functional states of the thalamus and the associated neuronal interplay. Physiological Reviews, 68(3), 649–742. https://doi.org/10.1152/physrev.1988.68.3.649 S

8. Subha, D. P., Joseph, P. K., Acharya U, R., & Lim, C. M. (2008). EEG Signal Analysis: A Survey. Journal of Medical Systems, 34(2), 195–212. https://doi.org/10.1007/s10916-008-9231-z

9. Britton JW, Frey LC, Hopp JLet al., authors; St. Louis EK, Frey LC, editors. & St. Louis EK. (2016). Electroencephalography (EEG): An Introductory Text and Atlas of Normal and Abnormal Findings in Adults, Children, and Infants. American Epilepsy Society,

10. Brain Basics: Understanding Sleep | National Institute of Neurological Disorders and Stroke, US National Institutes of Health. (2019, August 13). Retrieved October 18, 2019, from https://www.ninds.nih.gov/Disorders/Patient-Caregiver-Education/Understanding-Sleep

11. Parmeggiani, P. L., & A. Velluti, R. (2005). The Physiologic Nature of Sleep. London, UK: Imperial College Press.

12. Otmani, S., Pebayle, T., Roge, J., & Muzet, A. (2005). Effect of driving duration and partial sleep deprivation on subsequent alertness and performance of car drivers. Physiology & behavior, 84(5), 715–724. https://doi.org/10.1016/j.physbeh.2005.02.021

13. Liu, C. C., Hosking, S. G., & Lenné, M. G. (2009). Predicting driver drowsiness using vehicle measures: recent insights and future challenges. Journal of safety research, 40(4), 239–245. https://doi.org/10.1016/j.jsr.2009.04.005

14. Forsman PM, Vila BJ, Short RA, Mott CG, Van Dongen HP. Efficient driver drowsiness detection at moderate levels of drowsiness. Accid Anal Prev. 2013;50:341-350. DOI:10.1016/j.aap.2012.05.005

15. Thiffault, P., & Bergeron, J. (2003). The monotony of the road environment and driver fatigue: a simulator study. Accident; analysis and prevention, 35(3), 381–391. https://doi.org/10.1016/s0001-4575(02)00014-3

16. Sanei, S. (2013). Adaptive Processing of Brain Signals (1st ed.). West Sussex, UK: John Wiley & sons.

17. Bock, Thibaut & Das, Satyajit & Mohsin, M. & Munro, Nancy & Hively, Lee & Jiang, Yang & Smith, Charles & Wekstein, David & Jicha, Gregory & Lawson, Adam & Lianekhammy, Joann & Walsh, Erin & Kiser, S. & Black, Chelsea. (2010). Early detection of Alzheimer's disease using nonlinear analysis of EEG via Tsallis entropy. 10.1109/BSEC.2010.5510813.

18. Sahayadhas, A., Sundaraj, K., & Murugappan, M. (2012). Detecting Driver Drowsiness Based on Sensors: A Review. Sensors, 12(12), 16937–16953. https://doi.org/10.3390/s121216937

19 . Awais, M., Badruddin, N., & Drieberg, M. (2017). A Hybrid Approach to Detect Driver Drowsiness Utilizing Physiological Signals to Improve System Performance and Wearability. Sensors, 17(9), 1991. https://doi.org/10.3390/s17091991

20. Intelligent Transportation Systems Institute Center for Transportation Studies University of Minnesota, & Yu, X. (2009). Real-time Non-intrusive Detection of Driver Drowsiness. Retrieved from http://www.its.umn.edu/Publications/ResearchReports/pdfdownload.pl?id=1126

21. Lin, C.-T., Chang, C.-J., Lin, B.-S., Hung, S.-H., Chao, C.-F., & Wang, I.-J. (2010). A Real-Time Wireless Brain-Computer Interface System for Drowsiness Detection. IEEE Transactions on Biomedical Circuits and Systems, 4(4), 214–222. https://doi.org/10.1109/tbcas.2010.2046415

22. T. Azim, M. A. Jaffar, and A. M. Mirza, (2009). Automatic Fatigue Detection of Drivers through Pupil Detection and Yawning Analysis, Fourth International Conference on Innovative Computing, Information, and Control (ICICIC), Kaohsiung, 2009, pp. 441-445, DOI: 10.1109/ICICIC.2009.119.

23. Danisman, Taner & Bilasco, Ioan Marius & Djeraba, Chaabane & Ihaddadene, Nacim. (2010). Drowsy driver detection system using eye blink patterns. 2010 International Conference on Machine and Web Intelligence, ICMWI 2010 - Proceedings. 10.1109/ICMWI.2010.5648121.

24. Dongwook Lee, Seungwon Oh, Seongkook Heo, and Minsoo Hahn. (2008). Drowsy Driving Detection Based on the Driver's Head Movement using Infrared Sensors. In Proceedings of the 2008 Second International Symposium on Universal Communication (ISUC '08). IEEE Computer Society, USA, 231–236. DOI:https://doi.org/10.1109/ISUC.2008.76

25. American Epilepsy Society, & St. Louis EK. (2016). Electroencephalography (EEG): An Introductory Text and Atlas of Normal and Abnormal Findings in Adults, Children, and Infants. Retrieved from https://www.ncbi.nlm.nih.gov/books/NBK390346/

26. Berg, J., Neely, G., Wiklund, U., & Landstrom, U. (2005). Heart rate variability during sedentary work and sleep in normal and sleep-deprived states. Clinical Physiology and Functional Imaging, 25(1), 51–57. https://doi.org/10.1111/j.1475-097x.2004.00589.x

27. Snyder, F., Hobson, J. A., Morrison, D. F., & Goldfrank, F. (1964). Changes in respiration, heart rate, and systolic blood pressure in human sleep. Journal of Applied Physiology, 19(3), 417–422. https://doi.org/10.1152/jappl.1964.19.3.417

28. Tochikubo, O., Ikeda, A., Miyajima, E., & Ishii, M. (1996). Effects of Insufficient Sleep on Blood Pressure Monitored by a New Multibiomedical Recorder. Hypertension, 27(6), 1318–1324. https://doi.org/10.1161/01.hyp.27.6.1318. DOI:10.1161/01.hyp.27.6.1318

29. Sung, E. J., Min, B. C., Kim, S. C., & Kim, C. J. (2005). Effects of oxygen concentrations on driver fatigue during simulated driving. Applied Ergonomics, 36(1), 25–31. https://doi.org/10.1016/j.apergo.2004.09.003

30. Germ´ an Rodr´ıguez-Berm´udez∗ and Pedro J. Garc´ıa-Laencina∗ (2015) Analysis of EEG Signals using Nonlinear Dynamics and Chaos: A review Appl. Math. Inf. Sci. 9, No. 5, 2309-2321. http://dx.doi.org/10.12785/amis/090512

31. Tong, S., & Thankor, N. V. (2009). Quantitative EEG Analysis Methods and Applications (Engineering in Medicine & Biology). Norwood, US: Artech House.

32. S. Claesen and R. I. Kitney, (1994). Estimation of the largest Lyapunov exponent of an RR interval and its use as an indicator of decreased autonomic heart rate control, Computers in Cardiology, Bethesda, MD, USA, 1994, pp. 133-136, DOI: 10.1109/CIC.1994.470231.

33. Wolf, A., Swift, J. B., Swinney, H. L., & Vastano, J. A. (1985). Determining Lyapunov exponents from a time series. Physica D: Nonlinear Phenomena, 16(3), 285–317. https://doi.org/10.1016/0167-2789(85)90011-9

34. Stam, C. J. (2006). Nonlinear Brain Dynamics (1st ed.). NY, USA: Nova Biomedical.

35. Kantz, Holger & Radons, Günter & Yang, Hong-liu. (2013). The problem of spurious Lyapunov exponents in time series analysis and its solution by covariant Lyapunov vectors. Journal of Physics A: Mathematical and Theoretical. 46. 254009. 10.1088/1751-8113/46/25/254009.

36. Jelles, B., van Birgelen, J. H., Slaets, J. P. J., Hekster, R. E. M., Jonkman, E. J., & Stam, C. J. (1999). Decrease of nonlinear structure in the EEG of Alzheimer patients compared to healthy controls. Clinical Neurophysiology, 110(7), 1159–1167. https://doi.org/10.1016/s1388-2457(99)00013-9

37. Pesin, Y. B. (1977). Characteristic Lyapunov exponents and smooth ergodic theory. Russian Mathematical Surveys, 32(4), 55-114. https://doi.org/10.1070/RM1977v032n04ABEH001639

38. Grassberger, P. & Procaccia, I. (1983). Estimation of the Kolmogorov entropy from a chaotic signal. *Physical Review A* 28, 2591–2593, https://doi.org/10.1103/PhysRevA.28.2591.

39. PINCUS, S. M. (2006). Assessing Serial Irregularity and Its Implications for Health. Annals of the New York Academy of Sciences, 954(1), 245–267. https://doi.org/10.1111/j.1749-6632.2001.tb02755.x

40. Rosso, O. A., Blanco, S., Yordanova, J., Kolev, V., Figliola, A., Schürmann, M., & Başar, E. (2001). Wavelet entropy: a new tool for analysis of short duration brain electrical signals. Journal of Neuroscience Methods, 105(1), 65–75. https://doi.org/10.1016/s0165-0270(00)00356-3

41. Bruhn, J., Lehmann, L. E., Röpcke, H., Bouillon, T. W., & Hoeft, A. (2001). Shannon Entropy Applied to the Measurement of the Electroencephalographic Effects of Desflurane. Anesthesiology, 95(1), 30–35. https://doi.org/10.1097/00000542-200107000-00010

42. Yin, Y., Sun, K., & He, S. (2018). Multiscale permutation Rényi entropy and its application for EEG signals. PloS one, 13(9), e0202558. https://doi.org/10.1371/journal.pone.0202558

43. Abarbanel, H. (2012). Analysis of Observed Chaotic Data. New York, United States: Springer Publishing.

44. Fraser, A. M., & Swinney, H. L. (1986). Independent coordinates for strange attractors from mutual information. Physical review. A General Physics, 33(2), 1134–1140. https://doi.org/10.1103/physreva.33.1134

45. Fell, J., Mann, K., Röschke, J., & Gopinathan, M. S. (2000). Nonlinear analysis of continuous ECG during sleep I. Reconstruction. Biological Cybernetics, 82(6), 477–483. https://doi.org/10.1007/s004220050600

46. Moon, F. C. (1987). Chaotic Vibrations: An Introduction for Applied Scientists and Engineers (1st ed.). Sussex, UK: Wiley-VCH.

47. Wright, J., Kydd, R. & Liley, D. (1993). EEG models: chaotic and linear. *Psychology* 4, EEG–chaos.1. Wright.

48. Shahab Hasanzadeh Ghafari. (2007). A Fault Diagnosis System for Rotary Machinery Supported by Rolling Element Bearings, Thesis, Waterloo, Ontario, Canada,

49. Grassberger P. & I. Procaccia. (1983). Characterization of strange attractors *Physical Review Letters*, 50(5), 346-349. DOI: 10.1103/PhysRevLett.50.346.

50. Strogatz, S. H. (2019). Nonlinear Dynamics and Chaos: With Applications to Physics, Biology, Chemistry, and Engineering, Second Edition (2nd ed.). Philadelphia, US: West view Press.

51. Holden, A. V. (1986). Chaos-Nonlinear Science: Theory and Applications. Manchester, UK: Manchester University Press.

52. C Stam. J. (2005). Nonlinear dynamical analysis of EEG and MEG: review of an emerging field. Clinical neurophysiology: official journal of the International Federation of Clinical Neurophysiology, 116(10), 2266–2301. https://doi.org/10.1016/j.clinph.2005.06.011

53. Mining: Statistics and Facts. (2019, 11 2). Retrieved from Statista: https://www.statista.com/topics/1143/mining/

54. Ford, D. J., Ph.D. (2011, July 20). How the Brain Learns. Retrieved from https://trainingindustry.com/articles/content-development/how-the-brain-learns/

55. Niedermeyer, E., & da Silva, L. F., MD Ph.D. (2004). Electroencephalography: Basic Principles, Clinical Applications, and Related Fields (Fifth ed.). Philadelphia, USA: LWW.

56. N Sethi, P Sethi, J Torgovnick, E Arsura. (2006). Physiological and non-physiological EEG artifact. The Internet Journal of Neuromonitoring, 5(2), 3–8. Retrieved from http://ispub.com/IJNM/5/2/12498

57. Koseska, A., & Bastiaens, P. I. (2017). Cell signaling as a cognitive process. The EMBO journal, 36(5), 568–582. https://doi.org/10.15252/embj.201695383

58. Singh, M., & Kaur, S. (2012). Epilepsy detection using EEG an overview. International Journal of Information Technology and Knowledge Management, 6(1), 3–5. Retrieved from http://csjournals.com/IJITKM/PDF%206-1/Article_2.pdf

59. Stam, C. J., Pijn, J. P., Suffczynski, P., & Lopes da Silva, F. H. (1999). Dynamics of the human alpha rhythm: evidence for non-linearity?. Clinical neurophysiology: official journal of the International Federation of Clinical Neurophysiology, 110(10), 1801–1813. https://doi.org/10.1016/s1388-2457(99)00099-1

60. Krakovská, A. (2009). Two Decades of Search for Chaos in Brain. Measurement, 90–94. Retrieved from http://citeseerx.ist.psu.edu/viewdoc/download?doi=10.1.1.329.9632&rep=rep1&type=pdf

61. Callaway, E., & Harris, P. R. (1974). Coupling between cortical potentials from different areas. Science (New York, N.Y.), 183(4127), 873–875. https://doi.org/10.1126/science.183.4127.873

62. Guevara, M. R., Glass, L., Mackey, M. C., & Shrier, A. (1983). Chaos in neurobiology. IEEE Transactions on Systems, Man, and Cybernetics, SMC-13(5), 790–798. https://doi.org/10.1109/TSMC.1983.6313073

63. Faure, P., & Korn, H. (2001). Is there chaos in the brain? I. Concepts of nonlinear dynamics and methods of investigation. Comptes rendus de l'Academie des sciences. Serie III, Sciences de la vie, 324(9), 773–793. https://doi.org/10.1016/s0764-4469(01)01377-4

64. Simm, W.C. & Sawley, Mark & Skiff, Fred & Pochelon, Antoine. (1987). On the Analysis of Experimental Signals for Evidence of Deterministic Chaos. Helvetica Physica Acta, 60(4), 510–551. Retrieved from http://infoscience.epfl.ch/record/119197

65. Bassett, D. S., & Gazzaniga, M. S. (2011). Understanding complexity in the human brain. Trends in Cognitive Sciences, 15(5), 200–209. https://doi.org/10.1016/j.tics.2011.03.006

66. Kobayashi, T., Madokoro, S., Wada, Y., Misaki, K., & Nakagawa, H. (2001). Human sleep EEG analysis using the correlation dimension. Clinical EEG (electroencephalography), 32(3), 112–118. https://doi.org/10.1177/155005940103200305

67. Röschke, J., & Aldenhoff, J. B. (1992). A nonlinear approach to brain function: deterministic chaos and sleep EEG. Sleep, 15(2), 95–101. https://doi.org/10.1093/sleep/15.2.95

68. Fell, J., Röschke, J., & Beckmann, P. (1993). Deterministic chaos and the first positive Lyapunov exponent: a nonlinear analysis of the human electroencephalogram during sleep. Biological Cybernetics, 69(2), 139–146. https://doi.org/10.1007/BF00226197

69. Achermann, P., Hartmann, R., Gunzinger, A., Guggenbühl, W., & Borbély, A. A. (1994). Correlation dimension of the human sleep electroencephalogram: cyclic changes in the course of the night. The European journal of neuroscience, 6(3), 497–500. https://doi.org/10.1111/j.1460-9568.1994.tb00292.x

70. Achermann, P., Hartmann, R., Gunzinger, A., Guggenbühl, W., & Borbély, A. A. (1994). All-night sleep EEG and artificial stochastic control signals have similar correlation dimensions. Electroencephalography and clinical neurophysiology, 90(5), 384–387. https://doi.org/10.1016/0013-4694(94)90054-x

71. Röschke, J., & Aldenhoff, J. B. (1993). Estimation of the dimensionality of sleep-EEG data in schizophrenics. European archives of psychiatry and clinical neuroscience, 242(4), 191–196. https://doi.org/10.1007/BF02189962

72. Babloyantz A, Salazar JM, Nicolis C. (1985). Evidence of chaotic dynamics of brain activity during the sleep cycle. Phys Lett A 111(1) 152-156. https://doi.org/10.1016/0375-9601(85)90444-X

73. Acharya U, R., Faust, O., Kannathal, N., Chua, T., & Laxminarayan, S. (2005). Nonlinear analysis of EEG signals at various sleep stages. Computer methods and programs in biomedicine, 80(1), 37–45. https://doi.org/10.1016/j.cmpb.2005.06.011

74. Pereda, E., Gamundi, A., Rial, R., & González, J. (1998). Nonlinear behavior of human EEG: fractal exponent versus correlation dimension in awake and sleep stages. Neuroscience Letters, 250(2), 91–94. https://doi.org/10.1016/s0304-3940(98)00435-2

75. Mardi, Z., Ashtiani, S. N., & Mikaili, M. (2011). EEG-based Drowsiness Detection for Safe Driving Using Chaotic Features and Statistical Tests. Journal of medical signals and sensors, 1(2), 130–137.

76. Ma, Y., Shi, W., Peng, C. K., & Yang, A. C. (2018). Nonlinear dynamical analysis of sleep electroencephalography using fractal and entropy approaches. Sleep medicine reviews, 37, 85–93. https://doi.org/10.1016/j.smrv.2017.01.003

77. Jeong, J., Kim, S. Y., & Han, S. H. (1998). Nonlinear dynamical analysis of the EEG in Alzheimer's disease with optimal embedding dimension. Electroencephalography and clinical neurophysiology, 106(3), 220–228. https://doi.org/10.1016/s0013-4694(97)00079-5

78. The Parker Bay Company. (2020, January 29). *Mine Coverage and Equipment Database*. Retrieved January 29, 2020, from The Parker Bay Company: https://parkerbaymining.com/

79. Martell, M. (Feb 2018). Mine Worker Fatigue and Circadian Rhythms. *E&MJ*, 38-40.

80. Fraser, A. M., & Swinney, H. L. (1986). Independent coordinates for strange attractors from mutual information. Physical review. A General Physics, 33(2), 1134–1140. https://doi.org/10.1103/physreva.33.1134

81. Akay, M. (2000). Nonlinear Biomedical Signal Processing, Volume 2: Dynamic Analysis and Modeling (IEEE Press Series on Biomedical Engineering) (1st ed.). NY, USA: Wiley-IEEE Press.

82. R. P. Balandong, R. F. Ahmad, M. N. Mohamad Saad, and A. S. Malik, (2018) "A Review on EEG-Based Automatic Sleepiness Detection Systems for Driver," in *IEEE Access*, vol. 6, pp. 22908-22919, DOI: 10.1109/ACCESS.2018.2811723.

83. Eoh, H.J., Chung, M.K., Kim, S.-H.: 'Electroencephalographic study of drowsiness in simulated driving with sleep deprivation', Int. J. Ind. Ergon., 2005, 35, pp. 307–320 16 Jap, B.T., Lal, S., Fischer, P., Bekiaris, E.: 'Using EEG spectral components to assess algorithms for detecting fatigue', Expert Syst. Appl., 2009, 36, pp. 2352–2359

84. *Mandelbrot, Benoît B. (1983*). The fractal geometry of nature. Macmillan. ISBN 978-0-7167-1186-5.

85. Mandelbrot, Benoit B. (1967). "How long is the coast of Britain? Statistical self-similarity and fractional dimension". Science. New Series. 156 (3775): 636–638. Bibcode:1967Sci... 156..636M. doi:10.1126/science.156.3775.636. PMID 17837158. S2CID 15662830

86. Falconer, Kenneth (2003). *Fractal Geometry. Wiley. p. 308. ISBN 978-0-470-84862-3*

87. Rosana, E., George V., Javier, E., Brian L., (2001) A Comparison of Waveform Fractal Dimension Algorithms IEEE Transactions on Circuits And Systems—I: Fundamental Theory And Applications, Vol. 48, No. 2,

88. Datseris, G., Kottlarz, I., Braun, A., & Parlitz, U. (2021). Estimating the fractal dimension: a comparative review and open-source implementations.

89. Srdjan, Kesić., Sladjana, Spasić. (2016). Application of Higuchi's fractal dimension from basic to clinical neurophysiology: A review. Computer Methods and Programs in Biomedicine, 133:55-70. doi: 10.1016/J.CMPB.2016.05.014

90. Higuchi, T. Approach to an irregular time series on the basis of the fractal theory," Physica D, vol. 31, pp. 277–283, 1988.

91. Higuchi, T. (1988) Approach to an irregular time series on the basis of the fractal theory. Phys. D 31, 277–283

92. Yilmaz, A., Unal, G. (2020) Multiscale Higuchi's fractal dimension method. Nonlinear Dyn. 101, 1441–1455 https://doi.org/10.1007/s11071-020-05826-w

93. Liehr, L., Massopust, P. (2020). On the mathematical validity of the Higuchi method. Phys. D 402, 132265 https://doi.org/10.1016/j.physd.2019.132265

94. Wanliss, J. A., & Wanliss, G. E. (2022). Efficient calculation of fractal properties via the Higuchi method. *Nonlinear dynamics*, *109*(4), 2893–2904. https://doi.org/10.1007/s11071-022-07353-2

95. Accardo, A., Affinito, M., Carrozzi, M., & Bouquet, F. (1997). Use of the fractal dimension for the analysis of electroencephalographic time series. *Biological cybernetics*, *77*(5), 339–350. https://doi.org/10.1007/s004220050394

96. EZ Entropy: a software application for the entropy analysis of physiological time-series, Peng Li Li *BioMed Eng OnLine (2019) 18:30* https://doi.org/10.1186/s12938-019-0650-514

97. Lee, G. M., Fattinger, S., Mouthon, A. L., Noirhomme, Q., & Huber, R. (2013). Electroencephalogram approximate entropy influenced by both age and sleep. Frontiers in neuroinformatics, 7, 33. https://doi.org/10.3389/fninf.2013.00033

98. Borowska,M.(2016).Entropy-Based Algorithms in the Analysis of Biomedical Signals. Studies in Logic, Grammar and Rhetoric,43(1) 21-32. https://doi.org/10.1515/slgr-2015-0039

99. Chouvarda, I., Rosso, V., Mendez, M. O., Bianchi, A. M., Parrino, L., Grassi, A., Terzano, M., & Cerutti, S. (2011). Assessment of the EEG complexity during activations from sleep. *Computer methods and programs in biomedicine*, *104*(3), e16–e28. https://doi.org/10.1016/j.cmpb.2010.11.005

100. Chen, W.; Wang, Z.; Xie, H.; Yu, W. (2007) Characterization of surface EMG signal based on fuzzy entropy. IEEE Trans. Neural Syst. Rehabil. Eng., 15, 266–272.

101. Simons, S., Espino, P., & Abásolo, D. (2018). Fuzzy Entropy Analysis of the Electroencephalogram in Patients with Alzheimer's Disease: Is the Method Superior to Sample Entropy?. *Entropy (Basel, Switzerland)*, *20*(1), 21. https://doi.org/10.3390/e20010021

102. Nithin Nagaraj, Sutirth Dey, (2013) A new complexity measure for time series analysis and classification The European Physical Journal Special Topics 222(3-4) DOI:10.1140/epjst/e2013-01888-9

103. Bandt, C., & Pompe, B. (2002). Permutation entropy: a natural complexity measure for time series. *Physical review letters, 88 17*, 174102. DOI:10.1103/PhysRevLett.88.174102

104. Pesin, Y. B. (1997). *Dimension Theory in Dynamical Systems*. Chicago Lectures in Mathematics.

105. Amarantidis, L.C.; Abásolo, D. (2019). Interpretation of Entropy Algorithms in the Context of Biomedical Signal Analysis and Their Application to EEG Analysis in Epilepsy. *Entropy*, *21*, 840. https://doi.org/10.3390/e21090840

106. Cao, Y.; Tung, W.W.; Gao, J.B.; Protopopescu, V.A. (2004); Hively, L.M. Detecting dynamical changes in time series using the permutation entropy. Phys. Rev. E, 70, 7.

107. Staniek, M.; Lehnertz, K. (2008) Symbolic transfer entropy. Phys. Rev. Lett., 100, 158101. American Physical Society DOI =10.1103/PhysRevLett.100.158101

108. Avilov, O., Popov, A., Kanaikin, O., & Kyselova, O. (2012). Permutation Entropy Analysis of Electroencephalogram. *Signal*, 100, 200.

109. Nicolaou, N., & Georgiou, J. (2012). Detection of epileptic electroencephalogram based on Permutation Entropy and Support Vector Machines. *Expert Syst. Appl., 39*, 202-209.

110. Li, J., Yan, J., Liu, X., & Ouyang, G. (2014). Using permutation entropy to measure the changes in EEG signals during absence seizures. Entropy, 16(6), 3049– 3061.

111. T. Zhang, W. Chen, M. Li (2016). Automatic seizure detection of electroencephalogram signals based on frequency slice wavelet transform and support vector machine Acta Phys. Sin. -Ch. Ed., 65 (3) p. 038703

112. K. Yatindra, M.L. Dewal, R.S., Anand (2014). Epileptic seizures detection in EEG using DWT-based ApEn and artificial neural network Signal Image Video Process., 8 (7)

113. V. Srinivasan, C. Eswaran, N. Sriraam (2007). Approximate entropy-based epileptic EEG detection using artificial neural networks IEEE T. Inf. Technol. B, 11 (3) pp.

114. Akareddy, S. M., & Kulkarni, P. K. (2013). EEG signal classification for epilepsy seizure detection using improved approximate entropy. *International Journal of Public Health Science (IJPHS)*, 2(1), 23‑32

115. Liang, Z., Wang, Y., Sun, X., Li, D., Voss, L. J., Sleigh, J. W., Hagihira, S., & Li, X. (2015). EEG entropy measures in anesthesia. *Frontiers in computational neuroscience*, *9*, 16. https://doi.org/10.3389/fncom.2015.00016

116. Singh, S., Bansal, S., Kumar, G., Gupta, I., & Thakur, J. R. (2017). Entropy as an Indicator to Measure Depth of Anaesthesia for Laryngeal Mask Airway (LMA) Insertion during Sevoflurane and Propofol Anaesthesia. *Journal of clinical and diagnostic research: JCDR*, *11*(7), UC01–UC03. https://doi.org/10.7860/JCDR/2017/27316.10177 PMC5583804

117. E. Anderson, J.G. Jakobsson, (2004) Entropy of EEG during anaesthetic induction: a comparative study with propofol or nitrous oxide as sole agent British Journal of Anaesthesia, Volume 92, Issue 2, Pages 167-170, ISSN 0007-0912, https://doi.org/10.1093/bja/aeh036.

118. Liu Q, Ma L, Fan S, Abbod MF, Shieh J. (2018). Sample entropy analysis for the estimating depth of anaesthesia through human EEG signal at different levels of unconsciousness during surgeries https://doi.org/10.7717/peerj.4817

119. Swiderski, B., Osowski, S., and Rysz, A., (2005). Lyapunov Exponent of EEG Signal for Epileptic Seizure Characterization. Proceedings of the 2005 European Conference on Circuit Theory and Design. 2 (28):153–156

120. Watt RC, Hameroff SR. (1988) Phase space electroencephalography (EEG): a new mode of intraoperative EEG analysis. Int J Clin Monitor Comput; 5:3–13.

121. Widman G, Schreiber T, Rehberg B, Hoeft A, Elger CE. (2000) Quantification of depth of anesthesia by nonlinear time series analysis of brain electrical activity. Phys Rev E; 62:4898–903.

122. Van den Broek. PhD Thesis. University of Nijmegen; 2003.Simons S, Espino P, Abásolo D. Fuzzy Entropy Analysis of the Electroencephalogram in Patients with Alzheimer's Disease: Is the Method Superior to Sample Entropy? Entropy (Basel). 2018 Jan 3;20(1):21. doi: 10.3390/e20010021. PMID: 33265112; PMCID: PMC7512198.

123. Fan, M., Yang, A. C., Fuh, J.-L., & Chou, C.-A. (2018). Topological pattern recognition of severe Alzheimer’s disease via regularized supervised learning of EEG complexity. Frontiers in Neuroscience, 12, 685

124. Yang, A. C., Wang, S.-J., Lai, K.-L., Tsai, C.-F., Yang, C.-H., Hwang, J.-P., Lo, M.-T., Huang, N. E., Peng, C.-K., & Fuh, J.-L. (2013). Cognitive and neuropsychiatric correlates of EEG dynamic complexity in patients with Alzheimer’s disease. Progress in Neuro-Psychopharmacology and Biological Psychiatry, 47, 52–61.

125. Awais, M.; Badruddin, N.; Drieberg, M. (2017). A Hybrid Approach to Detect Driver Drowsiness Utilizing Physiological Signals to Improve System Performance and Wearability. Sensors, 17, 1991.

126. Hu, J. (2017). Automated Detection of Driver Fatigue Based on AdaBoost Classifier with EEG Signals. Front. Comput. Neurosci., 11, 72.

127. Zhang, C.; Wang, H.; Fu, R. (2013). Automated Detection of Driver Fatigue Based on Entropy and Complexity Measures. IEEE Trans. Intell. Transp. Syst., 15, 168–177.

128. Lau ZJ, Pham T, Chen SHA, Makowski D. (2022) Brain entropy, fractal dimensions and predictability: A review of complexity measures for EEG in healthy and neuropsychiatric populations. Eur J Neurosci.;56(7):5047-5069. doi: 10.1111/ejn.15800.

129. Costa, M. D., Goldberger, A. L., & Peng, C.-K. (2002). Multiscale entropy analysis of complex physiologic time series. Physical Review Letters, 89(6), 068102

130. H. Kobayashi, B.L. Mark, W. Turin, Probability, Random Processes and Statistical Analysis: Applications to Communications, Signal Processing, Queueing Theory and Mathematical Finance, Cambridge University Press, 2011.

131. Li, X.,Cui,S.,andVoss,L.J.(2008a).Using permutation entropy to measure the electroencephalographic effects of sevoflurane. *Anesthesiology* 109, 448.doi: 10.1097/ALN.0b013e318182a91b

132. Chen, W., Zhuang, J., Yu, W., and Wang, Z. (2009). Measuring complexity using FuzzyEn, ApEn, and SampEn. Med. Eng. Phys. 31, 61–68. doi:10.1016/j.medengphy.2008.04.005

133. Support Vector Machines, Ingo Steinwart, Andreas Christmann Springer 2008,

134. Vapnik, Vladimir Naumovich. Statistical Learning Theory. New York: Wiley, 1998.

135. Shaoda Yu, Peng Li, Honghuang Lin, Rohani, E., Gwan Choi, Botang Shao, Qian Wang, (2013). "Support Vector Machine Based Detection of Drowsiness Using Minimum EEG Features", Social Computing (SocialCom), 2013 International Conference on Social Computing, 827-835, 8-14

136. Awais M, Badruddin N, Drieberg M. (1991). A Hybrid Approach to Detect Driver Drowsiness Utilizing Physiological Signals to Improve System Performance and Wearability. Sensors. 2017; 17(9): https://doi.org/10.3390/s17091991

137. Belakhdar, I., Kaaniche, W., Djemal, R., & Ouni, B. (2018). Single-channel-based automatic drowsiness detection architecture with a reduced number of EEG features. *Microprocessors and Microsystems*, 58(2), 13–23 https://doi.org/10.1016/j.micpro.2018.02.004

138. Shalash, W.M. (2019) Driver Fatigue Detection with Single EEG Channel Using Transfer Learning. In Proceedings of the 2019 IEEE International Conference on Imaging Systems and Techniques (IST), Abu Dhabi, United Arab Emirates, pp. 1–6.

139. Z. Xiaohua, XU, R. Jian, and Z. Xingjian, (2013). “Discriminating Threshold of Driving Fatigue Based on the Electroencephalography Sample Entropy by Receiver Operating Characteristic Curve Analysis--Journal of Southwest Jiaotong University.

140. Anitha, C. (2019). Detection and analysis of drowsiness in human beings using multimodal signals. In: Digital Business, pp. 157–174.Springer, Heidelberg

141. Correa, A.G., Orosco, L., Laciar, E. (2014). Automatic detection of drowsiness in EEG records based on multimodal analysis. *Med. Eng. Phys.* **36**(2), 244–249

142. Mehreen, A.; Anwar, S.M.; Haseeb, M.; Majid, M.; Ullah, M.O. (2019). A Hybrid Scheme for Drowsiness Detection Using Wearable Sensors. IEEE Sens. J., 19, 5119–5126.

143. Hu, S.; Zheng, G.; Peters, B. (2013). Driver fatigue detection from electroencephalogram spectrum after electrooculography artifact removal. IET Intell. Transp. Syst., 7, 105–113

144. Picot, A.; Charbonnier, S.; Caplier, A. (2011). On-Line Detection of Drowsiness Using Brain and Visual Information. IEEE Trans. Syst. Man Cybern. Part A Syst. Hum. 42, 764–775.

145. Liu, J.; Zhang, C.; Zheng, C. (2010). EEG-based estimation of mental fatigue by using KPCA–HMM and complexity parameters. Biomed. Signal Process. Control. 5, 124–130.

146. Chaudhuri, A.; Routray, A. (2019). Driver Fatigue Detection Through Chaotic Entropy Analysis of Cortical Sources Obtained From Scalp EEG Signals. IEEE Trans. Intell. Transp. Syst. 21, 185–198.

147. Zou, S.; Qiu, T.; Huang, P.; Bai, X.; Liu, C. (2020) Constructing Multi-scale Entropy Based on the Empirical Mode Decomposition(EMD) and its Application in Recognizing Driving Fatigue. J. Neurosci. Methods, 341, 108691.

148. Correa, A.G., Orosco, L., Laciar, E. (2014). Automatic detection of drowsiness in EEG records based on multimodal analysis. Med. Eng. Phys. 36(2), 244– 249

149. Xiong Y, Gao J, Yang Y, Yu X, Huang W. (2016). Classifying driving fatigue based on combined entropy measure using EEG signals. *Int J Control Autom.* ;9(3):329–338. doi: 10.14257/ijca.2016.9.3.30.

150. Chai R, Naik G, Nguyen TN, Ling S, Tran Y, Craig A, et al. (2016). Driver fatigue classification with the independent component by entropy rate bound minimization analysis in an EEG-based system. IEEE Journal of Biomedical and Health Informatics.; PP(99):1±, https://doi.org/10.1109/JBHI 2016.2532354.